NASA TECHNICAL MEMORANDUM

NASA TM-82458

PROPULSION SYSTEM IGNITION OVERPRESSURE FOR THE SPACE SHUTTLE

By R. S. Ryan, J. H. Jones, S. H. Guest, H. G. Struck, M. H. Rheinfurth, and V. S. Verderaime

December 1981

NASA

George C. Marshall Space Flight Center
Marshall Space Flight Center, Alabama

TECHNICAL REPORT STANDARD TITLE PAGE

1. REPORT NO.	2. GOVERNMENT ACCESSION NO.	3. RECIPIENT'S CATALOG NO.
NASA TM-82458		

4. TITLE AND SUBTITLE	5. REPORT DATE
Propulsion System Ignition Overpressure for the Space Shuttle	December 1981
	6. PERFORMING ORGANIZATION CODE
7. AUTHOR(S) R. S. Ryan, J. H. Jones, S. H. Guest, H. G. Struck, M. H. Rheinfurth, and V. S. Verderaime	8. PERFORMING ORGANIZATION REPORT #
9. PERFORMING ORGANIZATION NAME AND ADDRESS	10. WORK UNIT NO.
George C. Marshall Space Flight Center Marshall Space Flight Center, Alabama 35812	11. CONTRACT OR GRANT NO.
	13. TYPE OF REPORT & PERIOD COVERED
12. SPONSORING AGENCY NAME AND ADDRESS	Technical Memorandum
National Aeronautics and Space Administration Washington, D.C. 20546	14. SPONSORING AGENCY CODE

15. SUPPLEMENTARY NOTES

Prepared by Systems Dynamics Laboratory, Science and Engineering

16. ABSTRACT

Liquid and solid rocket motor propulsion systems create an overpressure wave during ignition, caused by the accelerating gas particles pushing against or displacing the air contained in the launch pad or launch facility and by the afterburning of the fuel-rich gases. This wave behaves as a blast or shock wave characterized by a positive triangular-shaped first pulse and a negative half-sine wave second pulse. The pulse travels up the space vehicle and has the potential of either overloading individual elements or exciting overall vehicle dynamics. The latter effect results from the phasing difference of the wave from one side of the vehicle to the other. This overpressure phasing, or ΔP environment, because of its frequency content as well as amplitude, becomes a design driver for certain panels (e.g., thermal shields) and payloads for the Space Shuttle. This paper deals with the history of overpressure effects on the Space Shuttle, the basic overpressure phenomenon, Space Shuttle overpressure environment, scale model overpressure testing, and techniques for suppressing the overpressure environments.

17. KEY WORDS	18. DISTRIBUTION STATEMENT
	UNCLASSIFIED-UNLIMITED

19. SECURITY CLASSIF. (of this report)	20. SECURITY CLASSIF. (of this page)	21. NO. OF PAGES	22. PRICE
Unclassified	Unclassified	70	NTIS

TABLE OF CONTENTS

LIST OF ILLUSTRATIONS

LIST OF ILLUSTRATIONS (Continued)

LIST OF ILLUSTRATIONS (Concluded)

LIST OF TABLES

TECHNICAL MEMORANDUM

PROPULSION SYSTEM IGNITION OVERPRESSURE FOR THE SPACE SHUTTLE

INTRODUCTION

Although the first launch of the Space Shuttle vehicle was nearly flawless, the dynamic response of the Orbiter portion of the vehicle to ignition overpressure was greater than expected. Solid rocket motor ignition overpressure was a known phenomenon and considered in the design; however, although the amplitude was generally predicted, its frequency characteristics were less well defined, and there was no adequate determination of either the ΔP forcing function or the structural response of the vehicle to this function. Therefore, the correct response was not predicted. The initial environment was predicted using 6.4 percent scale model tests at Marshall Space Flight Center and full-scale Titan data. The unexpected high response of the first Shuttle flight vehicle to ignition overpressure dictated that a special effort be pursued to better understand the overpressure phenomenon and to devise an overpressure suppression technique for the second Shuttle flight, STS-2. This was accomplished through an inter-center and inter-industry ad hoc working group. This group defined potential fixes which were then tested in the Marshall Space Flight Center 6.4 percent scale model acoustic facility. Key parameters were identified, fixes defined and verified, full-scale environments developed, and vehicle response predicted to insure a safe second launch. This paper will address (1) a historic perspective of overpressure and pre-STS-1 prediction of environments, (2) STS-1 launch results, (3) overpressure characterization and scaling relationships, (4) special off-line tests to rank fixes, (5) 6.4 percent scale model tests to screen fixes, (6) 6.4 percent scale model tests of fixes and environment predictions, and (7) future considerations. There is very limited and sparse treatment of this subject in the open literature. In the following discussions, credit is given to the various individuals and their contributions. Most information obtained has been in the form of flight data, presentations to working groups, notes, and working papers, all of which have been shared unselfishly among those who worked the problem. This effort was greatly enhanced by the special support provided by the Huntsville-based Rockwell system support group, who furnished instrumentation plans, test plans, and data reduction and evaluation. Although we wish to acknowledge all contributions to this effort, it is possible that some were overlooked because of the vast amount of data involved.

6.4 PERCENT MODEL

Before proceeding with the main portion of the paper, it will be useful to describe the MSFC 6.4 percent scale model which played such a large role in the verification of potential fixes of the overpressure problem. The model was built as a 6.4 percent replica of the Space Shuttle during Shuttle Phase B design studies with the objective of understanding and suppressing the liftoff acoustic environments. The size was chosen based on available solid rocket motors that scaled the solid rocket motor (SRM) characteristics important to acoustics, such as exit velocity, thrust, and mass flow rate. Hot gas hydrogen and liquid oxygen scale model main engines were designed and used. All significant details of the Shuttle launch configuration, the Mobile Launch Platform (MLP), and the flame bucket were also duplicated. The facility has the capability of placing the vehicle in an elevated position relative to launch pad representing post-liftoff conditions so that maximum acoustical environments can be obtained. Figure 1 is a view of the 6.4 percent model and facility looking from the Orbiter side. The flame trench, MLP, and vehicle are clearly shown.

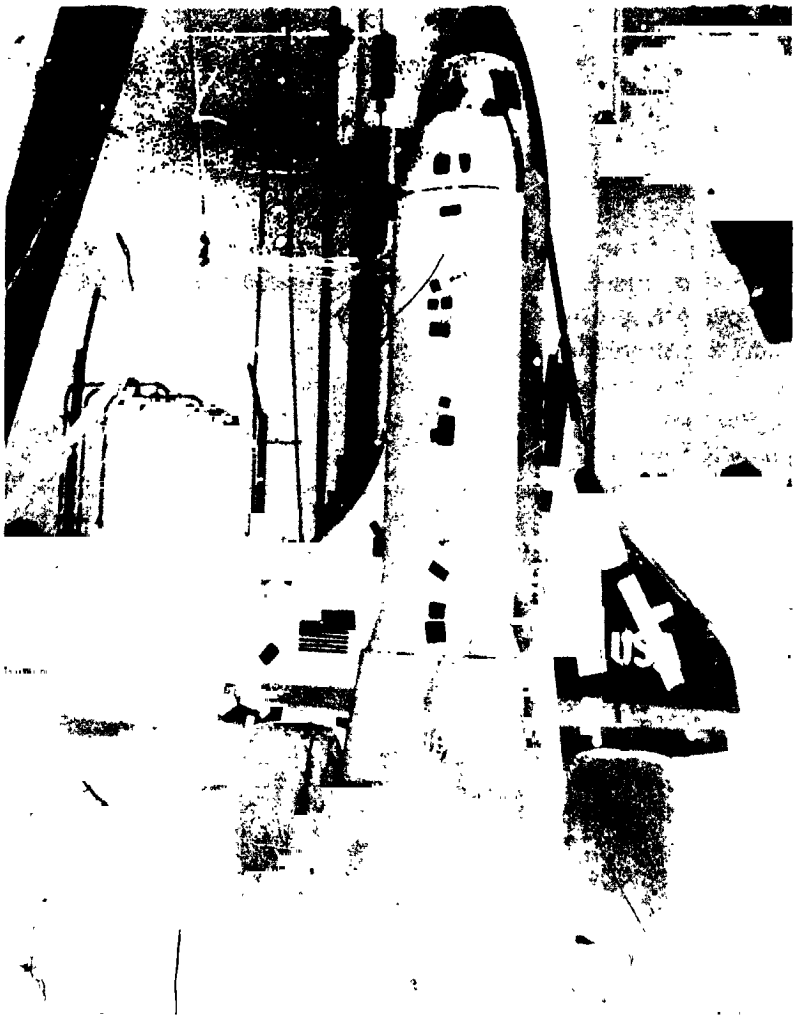

Figure 1. 6.4 percent model from Orbiter side.

Figure 2 shows a view of the facility and model from the side. Here, all vehicle elements are seen as well as the MLP. In addition to the 6.4 percent test program, the test stand has several other active test positions, a block house and instrumentation, control and data recording systems. The facility has a full contingent of engineers and technicians to support acoustic/overpressure and other ongoing test programs. Mechanical, instrumentation, and control personnel as well as machine and welding shops, photography, video, communications, etc., support the test activities as required. These facilities and personnel afford quick configuration changes and short test turnaround periods. Tests can be conducted at a frequency of up to one a day depending on the intermediate facility and model changes.

Not clearly seen in these pictures is the water system developed to suppress the liftoff acoustics. This system consists of a water spray at the top of the MLP from all sides of the SSME hole, spray into both the SSME and SRB plumes from the crest of the main deflector in the exhaust trench, water into the SRB drift hole from the east and west sides along the top of the flame trench, and water from six pedestals on top of the MLP to suppress acoustics caused by plume impingement on top of the MLP. The SRB drift hole was put in the MLP to reduce plume impingement and the resulting acoustics in the case of drift soon after liftoff. Figure 3 shows a view of the scale model with the water flowing.

Figure 2. 6.4 percent model from side.

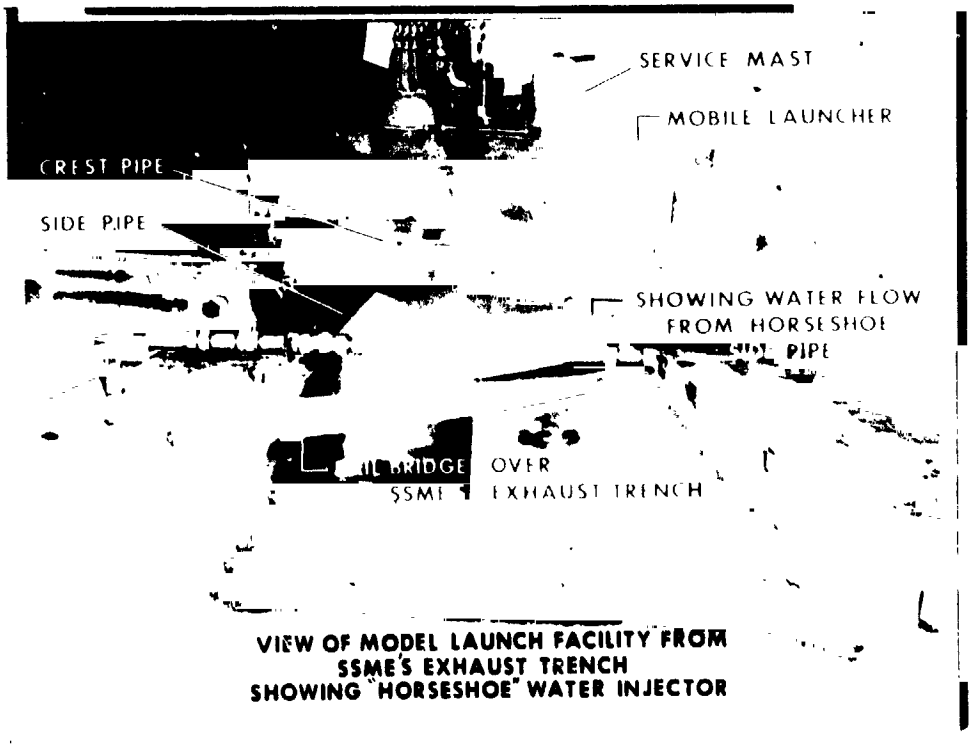

Figure 3. 6.4 percent STS-1 water system.

The value of this type of facility and the supporting personnel cannot be overestimated. In addition to the test personnel and facilities, there are supporting data reduction and data evaluation personnel and dynamic analysts who make up the remainder of a multidisciplinary team.

SECTION I. BACKGROUND AND OVERPRESSURE CHARACTERISTICS

A. History of Overpressure for Space Shuttle

In the mid-1970's, dynamics personnel from MSFC were involved in the solution of a combined pogo and payload loads problem for the Titan Viking launch. During these reviews, it was pointed out that one potential cause of the liftoff loads for the Titan Viking was the SRM ignition overpressure. As it turned out, this was not the cause of the liftoff loads for the Titan Viking. However, the large values observed, 8 to 10 psi, started a large effort to determine if overpressure was a problem for Space Shuttle. This activity was started in July 1975 under the auspices of the Level II Space Shuttle Loads Panel.

The first activity was to review analytical and experimental data available. In addition to the Titan data, it was found that The Boeing Company had run 1/20 scale model tests on the Minuteman and correlated them with full-scale data. General Dynamics had also conducted 1/30 scale model tests of the Atlas [1].

Because Air Force solid rockets are fired in silos, overpressure environments were a prime concern. A one-dimensional approach by Broadwell and Tsu [2] was developed to study this problem. This was simplified by considering the silo as a semi-infinite tube. This model and the Scott and Ried model [3], developed somewhat later, will be discussed in more detail later Both were used as a basis for studying the Shuttle overpressure problem. Some of the key people in this early work were Tom Modlin, Alden Mackey, Dr. Bob Ried, and Carl Scott of JSC; Jess Jones and Stan Guest of MSFC; and Fred Laspesa, Sam Krause, and Dr. Shih-li Lai of Rockwell International.

In the fall of 1975, it was decided that the MSFC 6.4 percent acoustic scale model be investigated as a potential for determining Space Shuttle overpressure environments. The MSFC 6.4 percent model was conceived and developed to investigate Shuttle acoustic environments and their suppression techniques. The model scale was chosen to fit available Tomahawk motors for the solid rocket motors, which from an acoustical standpoint were matched to the Space Shuttle SRM's. Hot gas hydrogen and liquid oxygen propulsion engines were developed to a 6.4 percent scale of the Shuttle liquid main engines. At this time, two key SRM parameters were understood to be important in the simulation of overpressure: chamber pressure, P_c, and pressure rise rate, $\dot{P}_c$. Thiokol's Tomahawk motors matched well the initial predicted characteristics of the Shuttle SRM's steady-state pressure and pressure rise rate. At the beginning of the SRM development and qualification firings, it was found that the Shuttle SRM's thrust rise rates were a factor of two higher than predicted, which required a change in scale model test planning.

Overpressure tests were run on the 6.4 percent scale model from December 1975 through March 1976. In addition, a 6.4 percent horizontal single motor firing was conducted to use as a comparison to the full-scale SRM developmental firings. Data also were obtained from two full-scale Titan firings, which were instrumented for overpressure. The 6.4 percent model was showing 4 psi at the top of the MLP, while the Titan data showed around 9 psi.

During this time period, several concerns were raised:

1. The effects of P_c, P_c rise rate, and other motor parameters
2. The proper scaling functions
3. The variability in data.

As a result of these concerns, a comprehensive analytical and experimental effort was proposed by MSFC in May 1976 to systematically evaluate these key parameters. This proposal was not funded, since the overpressure environments were not impacting the Shuttle element interface loads, which were the loads driven by the liftoff event at this stage of Shuttle development. It should be pointed out that whatever the current problems are, all activities are focused on that area; this emphasis results in overlooking other key areas. During the 1975 timeframe, the inter-element interfaces and their element backup structure were extremely sensitive to small parameter changes, such as SRM thrust mismatch, rise rate, and misalignment, and forced a costly redesign of this structure. Since the overpressure environment did not have a major influence on these loads, it was inadvertently assumed to be insignificant to all the Shuttle subelements.

Additional model tests were run in December 1976 to better define the overpressure environment. These tests resulted in an SRB thermal curtain overpressure design value of 6 psi, and confirmation of the original values obtained in 1975. In this timeframe, it became clear that a better understanding of scaling was required. This was particularly evident when a large scatter (factor of two) was observed in the Titan data. As a result, a scale model firing (7.5 percent) of the Titan was made in the MSFC facility. The Titan launch facility and vehicle were modeled for this test. Three of these tests were run in the summer of 1977. The results, compared with full-scale Titan data, showed that, for the Titan configuration, an empirical scale factor of approximately two was required for the model results to match full-scale results. This scale factor was adopted for the Shuttle.

The first Shuttle SRM development firing was conducted in November 1977. This firing showed the SRM P_c rise rate to be approximately a factor of two higher than predicted. This meant that the Tomahawk no longer scaled to the SRM. Scale model environment data must also be corrected for rise rate differences, and the Broadwell and Tsu model indicated that a factor of two was required for rise rate adjustment. A similar but less restrictive approach by Scott and Ried indicated that the adjustment for rise rate should be approximately 1.7. The Scott and Ried approach was subsequently used by Rockwell as the corrections for rise rate. Thiokol made an unsuccessful attempt to reduce the rise rate by modifying the igniter grain. Using the factor of 1.7 for rise rate scaling (an additional factor of 2 for a scaling adjustment indicated by Titan model/full-scale results) and scatter in the model data resulted in high predicted overpressure environments. Liftoff loads based on this environment resulted in design exceedances between 20 and 200 percent (March 1978). With these large load exceedances, it was decided that redesign to accommodate the load increases was not practical. The Loads Panel, under the guidance of JSC (Tom Modlin and Alden Mackey), convened all known people with overpressure experience and initiated a study of suppression techniques. Methods considered were hard covers on holes in the MLP, water injection, baffles in MLP, and soft covers over holes in MLP. Again, questions were raised concerning the understanding of the key parameters in the overpressure phenomenon and scaling uncertainties. In May 1978, before these suppression concepts could be evaluated, an error was found in the liftoff loads simulation in how the overpressure phasing with the liftoff twang was considered. Eliminating this error again showed overpressure to be a small contributor to vehicle loads, as well as the Orbiter heat shield and the SRB thermal curtain. This removed the urgency on the design of suppression devices, and this effort was dropped. In retrorespect, this large sensitivity to small changes should have been a key concern, and should have been given a more in-depth consideration.

The SRB thermal curtain was in final design in August 1978. The overpressure environment was revisited and again assessed to be between 5 and 6 psi on the SRB thermal curtain.

As the Shuttle moved toward final verification, it was decided to run some additional tests to obtain better overpressure characteristics. These tests were run without firing the SSME's to remove the extraneous noise from the data. There were differing opinions on how to treat overpressure and analyze the data from the tests. The issue was settled at this time by running loads and again showing the interface loads to not be sensitive to overpressure environments. In retrospect, the amplitudes of the overpressure were fairly accurately predicted by Guest as seen in Figure 4. However, no attempt was made to adjust the overpressure frequency for P_c rise rate effects; this meant that the frequency was underpredicted by about 40 percent: 4 Hz from model test data versus 6 Hz from STS-1 full-scale data.

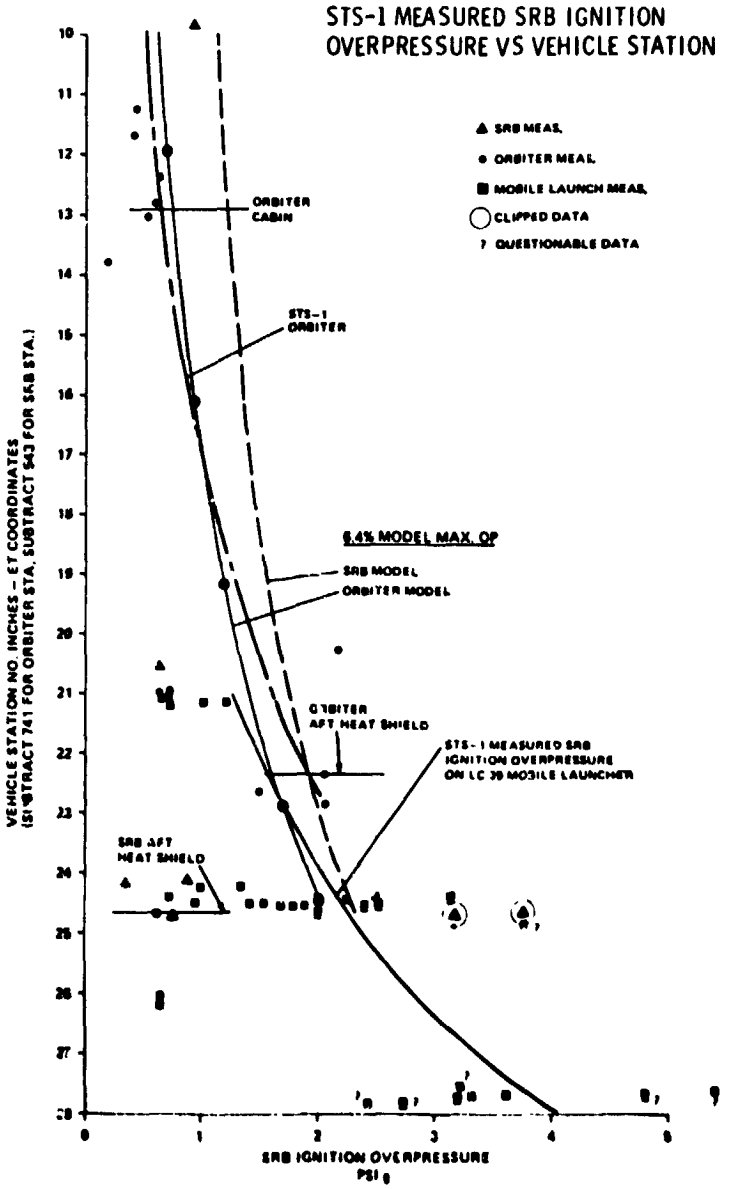

Figure 4. Overpressure amplitude predictions from 1978 model tests versus STS-1 measured.

One final review was made of the overpressure environment by the Williams committee in April 1980. This group also raised concerns over the data analysis methods and overpressure levels. As a result, loads were reassessed and an additional factor of two (increase) was placed on the amplitude (Titan experience). Again, no load exceedances (interfaces) were found; and the issue was closed.

With this brief history as background, the following section addresses the basic results of the STS-1 launch.

B. STS-1 Overpressure Characteristics

As stated in the introduction, the first Space Shuttle reusable space vehicle was launched in what appeared to be a flawless launch. In general, this was the case. Performance was good. Element interface loads were near-normally predicted. A detailed evaluation of the data, however, showed some surprises. The response of the vehicle to ignition overpressure, in particular the Orbiter, caused much concern. In fact, the overpressure environment on the Orbiter heat shield was near its design value of 1.8 psi, and the Orbiter response at various locations was approximately 80 percent of design values.

To put these concerns in perspective, it is necessary to look first at the vehicle's liftoff configuration and sequence. The Shuttle is placed on the Mobile Launcher (ML) on the four pedestals in each SRB exhaust hole, and is provided holddown constraints until SRB ignition. The launch platform and trenches serve to direct the propulsion system gases down and away from the Shuttle vehicle. The SSME propulsion gases are directed to one side and the SRB gases to the other using a flame deflector. Figure 5 shows a side view of the gas trenches, ML, and holddown pedestals (support posts).

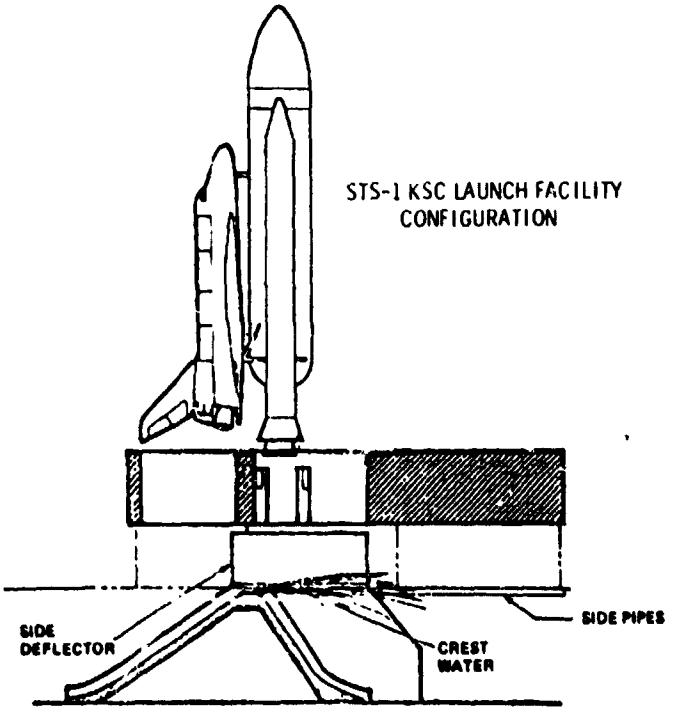

Figure 5. Side view of launch facilities and vehicle.

The flame deflector has large water-spray heads, spraying water into each exhaust gas plume, put in for cooling and reduction of acoustics environments. Looking down on top of the MLP (Fig. 6), we see the SSME exhaust gas hole on the left and two rectangular holes on the right for each SRB exhaust gases. The holddown and vehicle support pedestals can be seen near the left side of the SRB holes. The open areas to the right of these pedestals are there to keep the SRB exhaust gases from impinging on the MLP as the vehicle drifts during liftoff and from aggravating the acoustical environments.

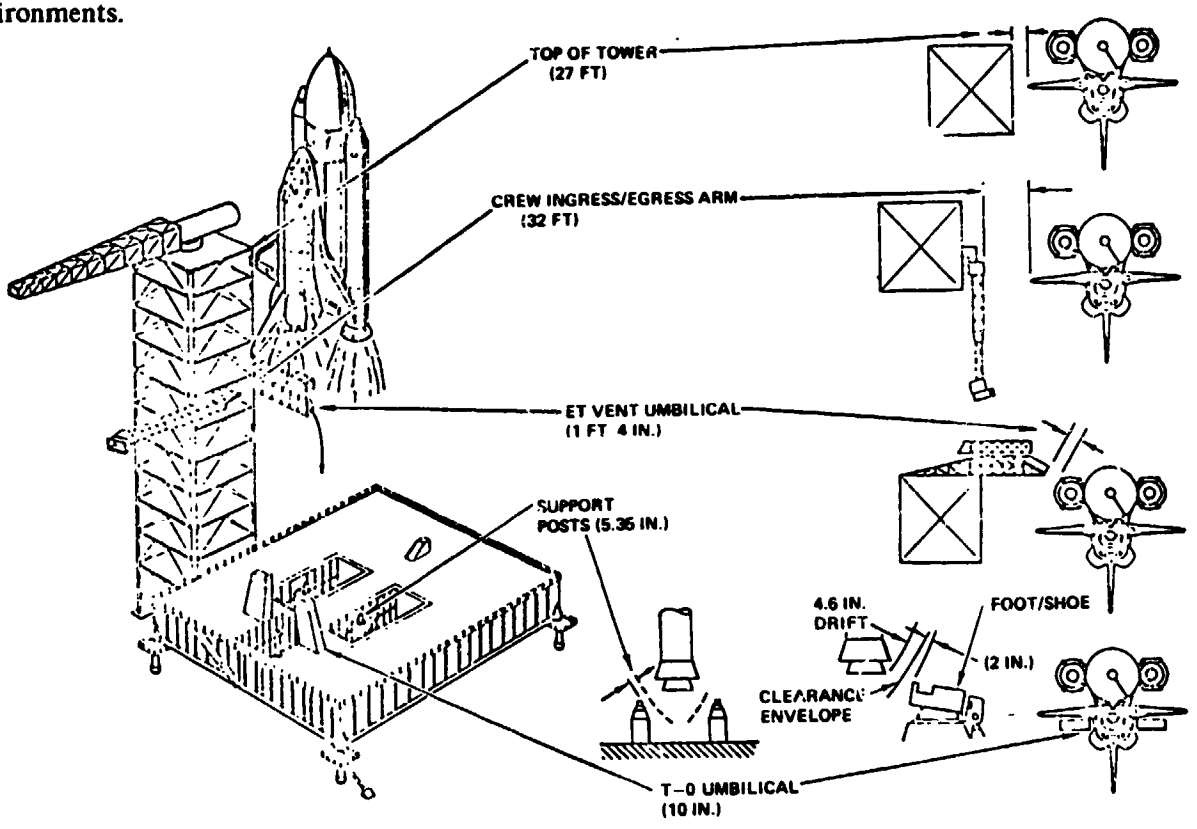

Figure 6. View on top of MLP.

The SSME hole has water injected around the top of the MLP into the SSME plumes to reduce acoustical environments. The same is true of the SRB holes for STS-1, except the water is injected lower, near the top of the flame trenches.

Obviously, these trenches and the ML act to contain and direct the propulsion system exhausts. This containment of the accelerating exhaust gas creates the overpressure phenomenon. In general, the accelerating exhaust gases push the contained air (piston effect) and overrun the initial particles, setting up a blast or shock wave which then propagates out of the exhaust plume holes and strikes the vehicle. This phenomenon will be discussed in more detail in a later section. Obviously, this overpressure is a function of the start-up characteristics of the propulsion system and, therefore, couples strongly with the total liftoff environment.

The liftoff sequence is as follows: The SSME's are started and throttled up to rated power level and held there for approximately 3 sec. Figure 5 shows that the SSME thrust is offset, and thus bends the vehicle over the SRB's and the holddown pedestals. A large base bending moment is created, which is relieved as the vehicle dynamically swings back. At the time this moment is minimum, the SRB ignition command and holddown bolt release command is given; and the liftoff sequence begins (Fig. 7).

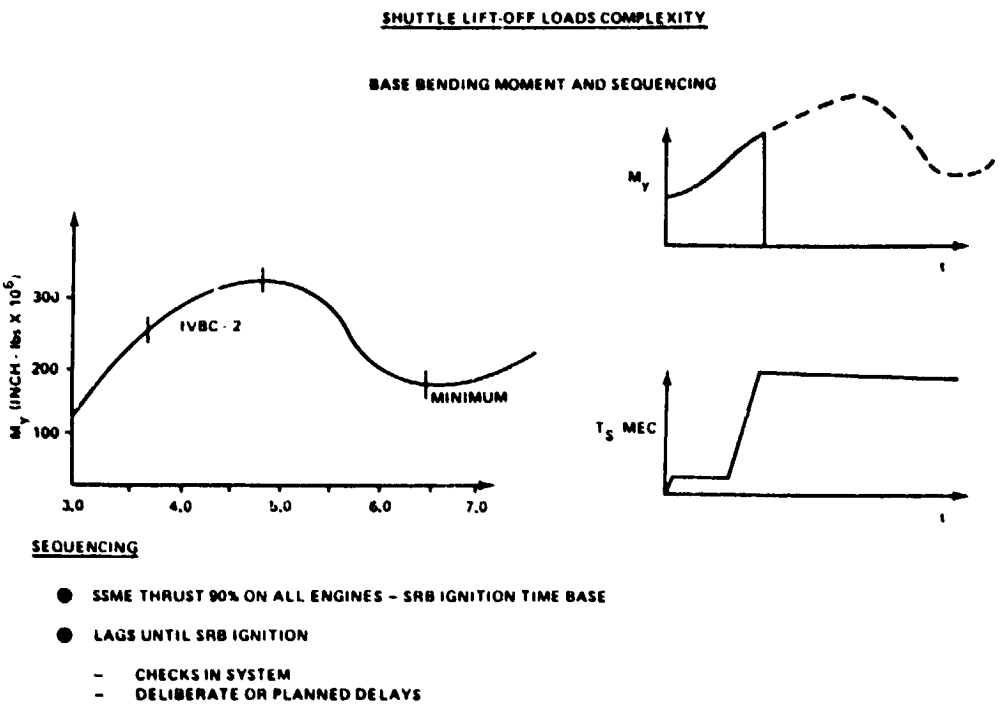

Figure 7. Base bending moment versus time.

At approximately 0.2 sec after the SRB ignition command, the overpressure waves emanate from the exhaust holes; and then, the first vertical motion of the vehicle occurs. The resulting dynamic loads [4] are a function of the SSME induced moment, SRM thrust, thrust rise rate, thrust difference between the SRM's, and the overpressure. Also important are thrust vector misalignments, winds, and the vehicle elastic body characteristics. Obviously, the overpressure environment-induced response combined to some extent with the liftoff twang load, creating larger responses.

Looking at the STS-1 environments and responses in terms of these sequences and the overall environment characteristics, it is clear that everything was nominal except the predicted overpressure response. Table 1 gives the predicted vehicle interface loads for a nominal vehicle compared to STS-1 flight values. Clearly, the basic vehicle and its loads were near nominal.

This analogy does not hold, however, for the Orbiter response. Figure 8 shows that the Orbiter elevon response is approximately 80 percent of design values. The response is basically an Orbiter mode with the Orbiter/ET attachments serving as node points.

Launch films of the elevons clearly show this response and that it occurred before the first liftoff motion. The same type of response occurred along the Orbiter centerline in the pitch plane, creating potential adverse payload response environments. Figure 9 is a typical plot for one of these responses.

Plotting the measured overpressure environment and comparing it to the response clearly shows that the overpressure caused the major portion of Orbiter response. Figures 10 and 11 are typical examples of two of these overpressure and resultant vibration measurements.

TABLE 1. INTERFACE LOADS

	Δ PREDICTED LOAD* (KIPS)	Δ MEASURED LOAD (KIPS) MEAN	PREDICTED NET LOAD (KIPS)	MEASURED NET LOAD (KIPS) MEAN	DESIGN LIMIT LOADS COMP/TEN
P1	− 74	− 62	− 58	− 46	−131/130
P2	− 74	− 57	− 58	− 41	−131/130
P3	254	223	183	152	−295/476
P4	254	221	183	150	−327/474
P5	−653	−666	−536	−548	−834/172
P6	−653	−609	−536	−490	−834/172
P7	− 28	− 4	− 28	− 4	−173/177
P8			−119	− 94	−306/393
P9			143	140	−306/393
P10			−112	−165	−306/393
P11			−119	−100	−306/393
P12			143	140	−306/393
P13			−112	−190	−306−393

*R/I V5.8 NOMINAL STS−1 LIFT−OFF CONDITION (L0796)

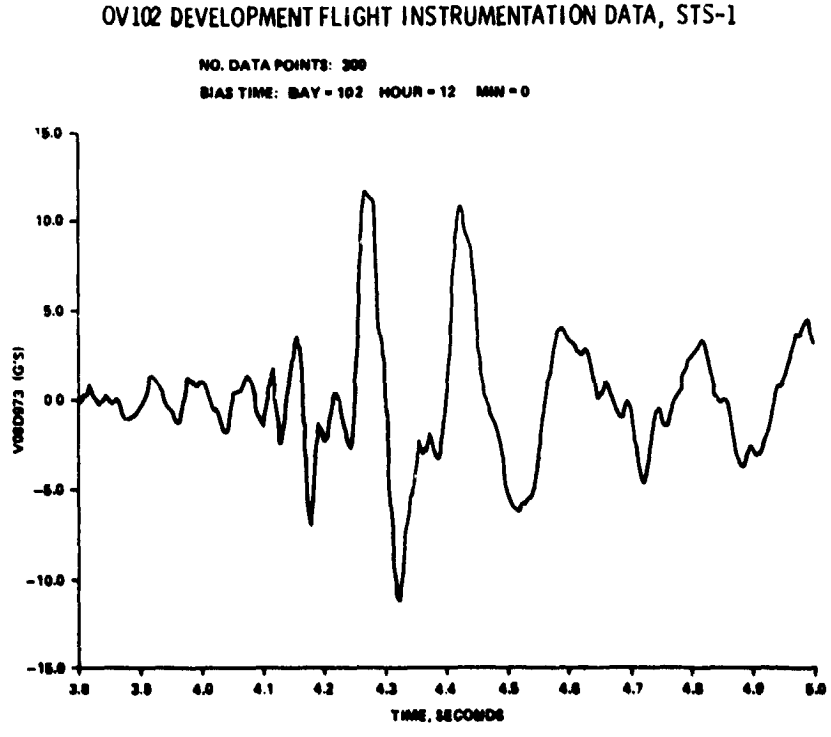

Figure 8. Orbiter elevon response.

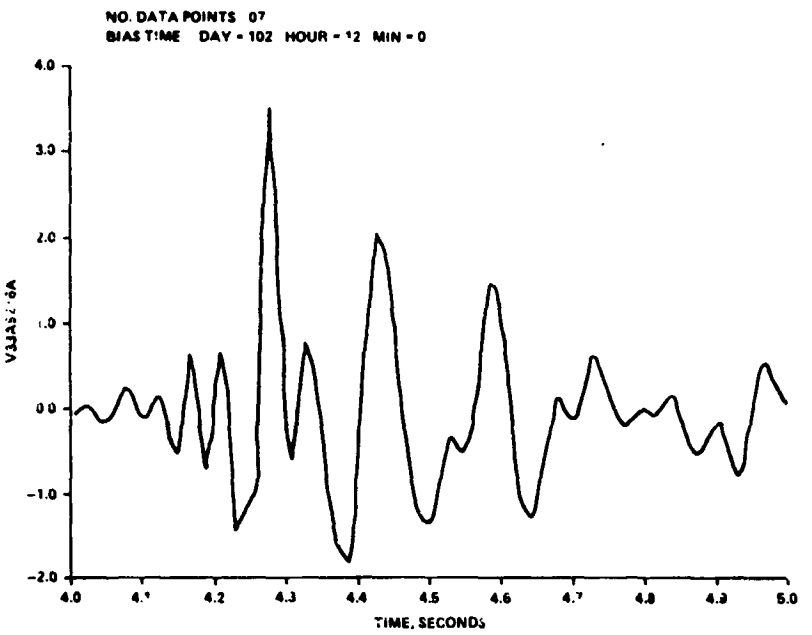

Figure 9. Orbiter response (pitch plane).

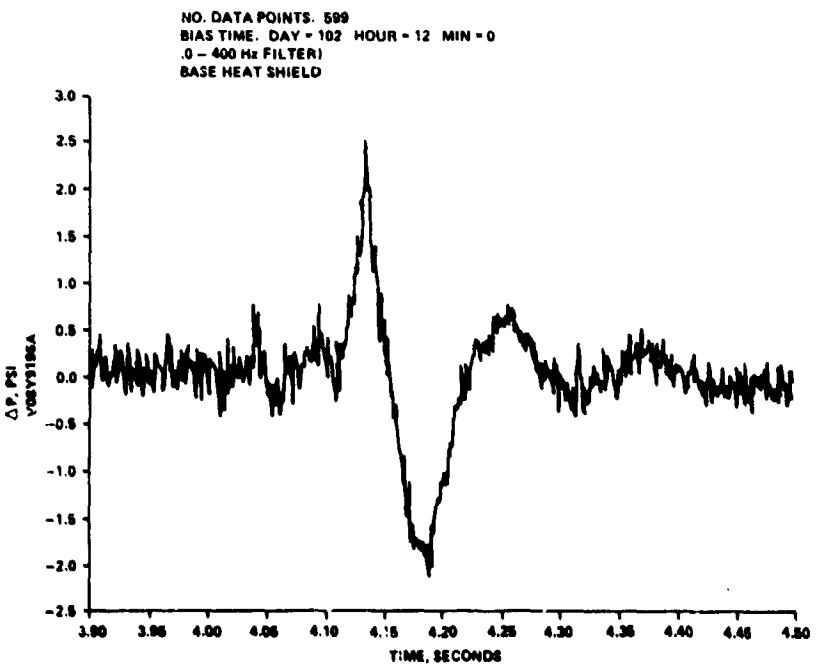

Figure 10. STS-1 Orbiter heat shield.

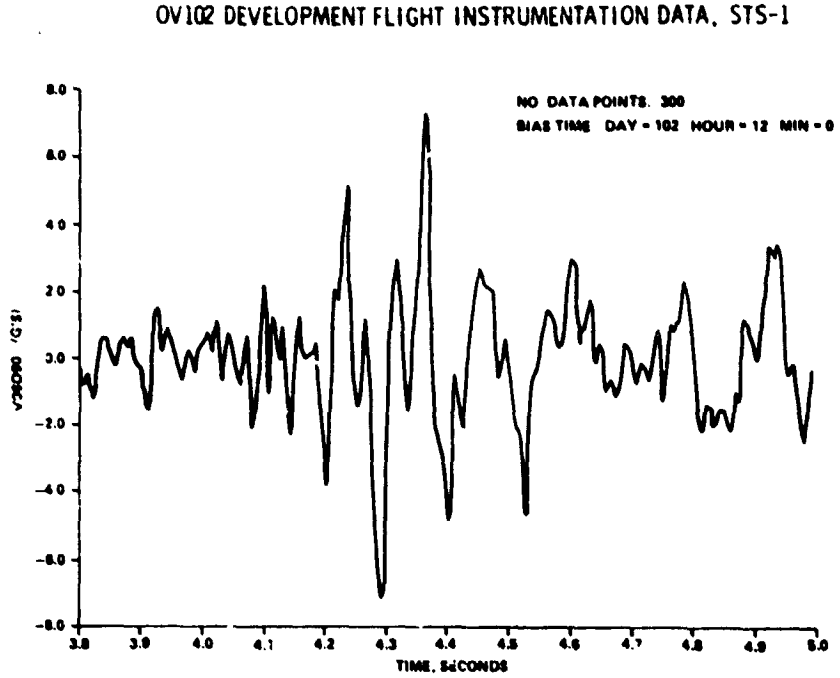

Figure 11. STS-1 Orbiter body flap.

Clearly, the SRM ignition overpressure is a problem to the Space Shuttle and its payloads.

Detailed evaluations were made by MSFC of the facility and vehicle overpressure data, timelines, and launch movies to obtain a better understanding of the overpressure characteristics. Each overpressure instrument and its response were time correlated to the liftoff event. The apparent source location of the overpressure wave was obtained by assuming source locations and fitting the distance and arrival time using a linear regression analysis. The results of this evaluation showed the apparent source location of the overpressure wave to be midway between the two SRM's and slightly biased to the outside of the SRB centerlines. Figure 12 shows this source reconstruction.

The facility measurements, which were treated separately from the Orbiter measurements, gave similar results. This evaluation also showed that the overpressure wave velocity was very near (slightly higher than) the speed of sound, indicating that the wave was behaving somewhat like a weak shock wave. Early analysis of the flight data conducted by Bob Ried and Carl Scott of JSC indicated that the wave approximated a blast wave in the MLP and on the lower vehicle and looked like a weak shock on the upper part of the vehicle. Figure 13 shows how the data fit different powers of the inverse of the distance (R). Further refinement of the data changed this correlation somewhat to more nearly fit an iso-intropic gas dynamics model (Section IV and Appendix C).

Theories such as Broadwell and Tsu developed in the early 1960's showed a dependence of the overpressure environment on the chamber pressure rise rate. Doug Blackwell and Steve Richards (MSFC) reconstructed the P_c rise rate for both STS-1 SRM's and for the QM-1 firing (qualification motor firing). Figure 14 is a plot of these rise rates.

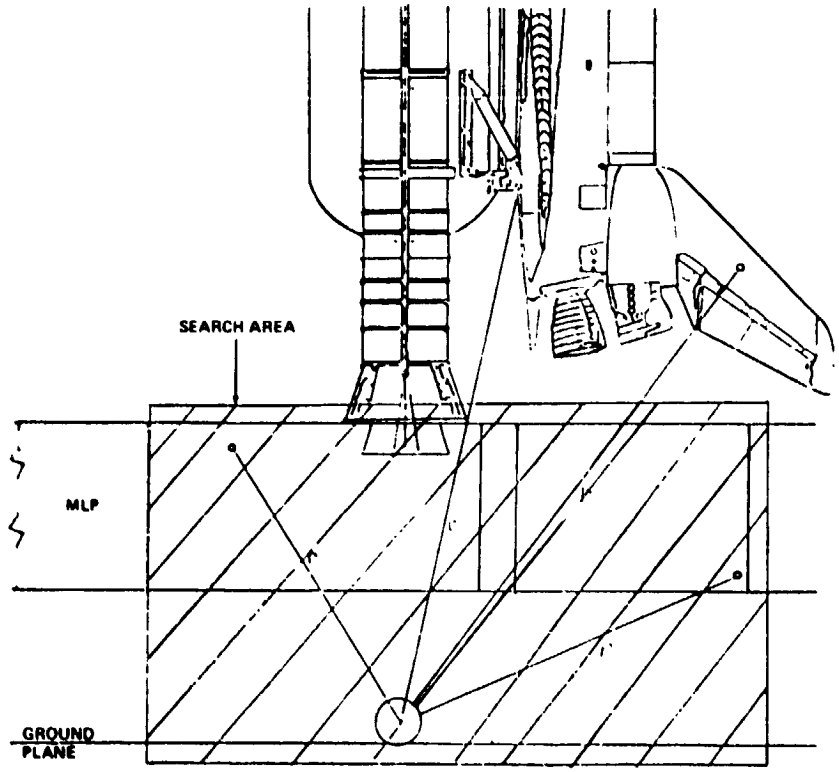

Figure 12. Apparent source of overpressure wave for STS-1 configuration.

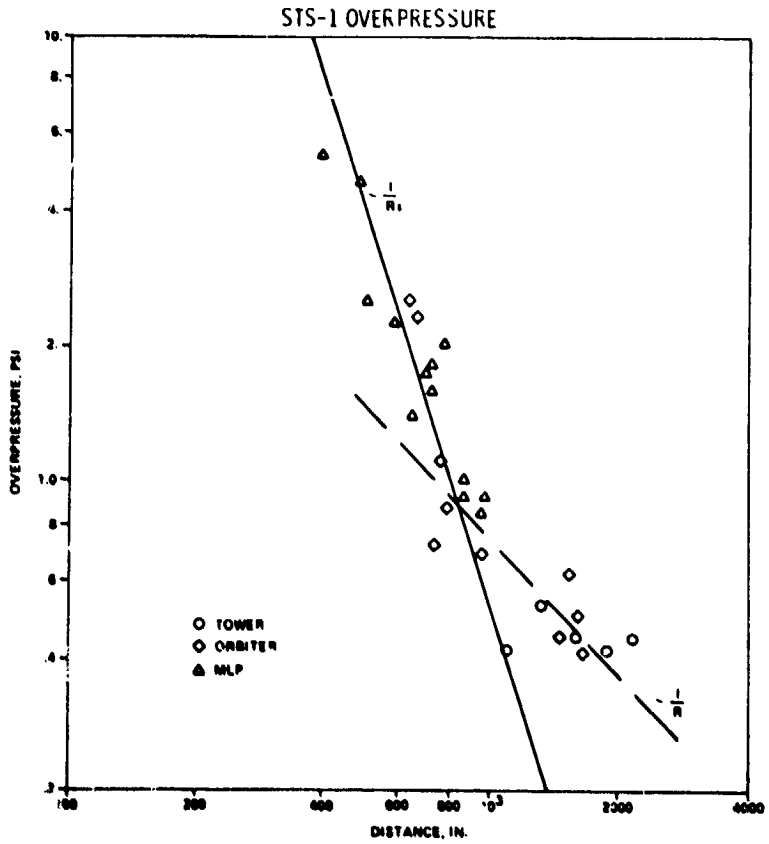

Figure 13. Overpressure versus distance from source.

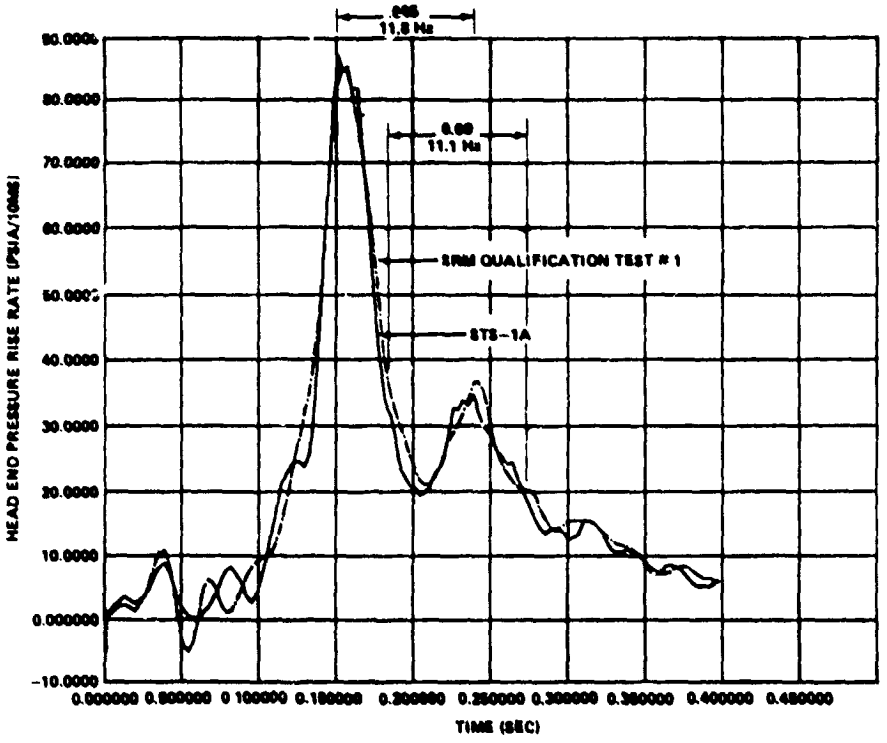

Figure 14. Comparison of the STS-1 and the SRM qualification motor test No. 1 ignition overpressure rise rate history.

Comparing the following plot (Fig. 15) of a typical overpressure measurement shows that the overpressure environment in both frequency and relative amplitude generally tracks the initial P_c rise rate ($\dot{P}_c$). Notice that the $\dot{P}_c$ curves have a very large spike followed by a smaller spike with a frequency around 6 Hz. The overpressure waves follow the first of these two positive spikes, nearly triangular in shape; however, the response to the second is barely visible, around 155 ms. The first peak is followed by a large, negative sine wave-type response, which is typical of weak blast waves. In summary, the first $\dot{P}_c$ spike dominates the overpressure wave, determining its general characteristics. As pointed out in the history section, the overall amplitude was adequately predicted (Fig. 4). No attempt was made to adjust the frequency of overpressure wave, i.e., approximately 4-Hz model compared with approximately 6-Hz on STS-1. In retrospect, this slightly lower frequency, though not significantly different from 6 Hz, was used in a loads model that resulted in inadequate vehicle response simulation. With the complex liftoff sequence of events, complex vehicle dynamic characteristics, and the large number of key system parameters in the vehicle response, this is not an unexpected result.

The results of the STS-1 launch led to the formation of an ad hoc working group chaired by Enoch Jones (JSC) with the objective of finding a fix for STS-2 without causing a schedule slip. Robert Ryan led the MSFC activities, Bill Frohoff led Rockwell activities, Jim Greenwood led KSC activities, and Bill Hamby led NASA Headquarters activities. Experts at all the above organizations, along with Thiokol, Aerospace, Martin, and special consultants, were a part of the working group; Rockwell had several key system personnel on-site to support the test. Sam Dougherty led their activities. All organizations sent people to MSFC at various times for special support. Two face-to-face meetings were held in conjunction with a daily telecon among all concerned. The telecon proved to be a very effective mechanism for handling this special problem. MSFC formed a special team to

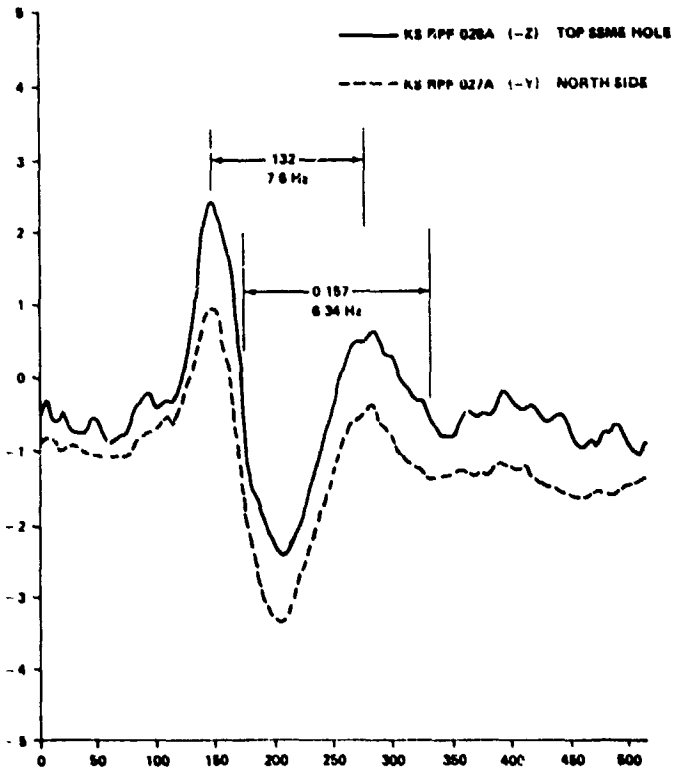

Figure 15. Overpressure versus time.

support this activity and take an independent systems look at all data, approaches, etc. The team, under the leadership of Bob Ryan, was composed of Doug Lamb, Structures; Bill Rhiel, Materials; Vince Verderaime, Stan Guest, and Jess Jones, Dynamics; Jim Ralston, Test; Terry Greenwood and Heinz Struck, Flow Environments; and Jim Igou, Shuttle Project Office. On-site Thiokol and Rockwell personnel supported this independent activity. The next section deals with the basic overpressure characteristics as theorized by various individuals.

C. Overpressure Characteristics and Scaling Laws

Five individual theories or models have been developed to understand the basic overpressure and to develop the scaling laws. These are: (1) one-dimensional model of the SRB igniter pulse, plug rupture, and overpressure wave generation, Dr. Lai, Rockwell International; (2) simplified Broadwell/Tsu one-dimensional model of overpressure wave generation, Jess Jones, MSFC; (3) one-dimensional model of the igniter shock and overpressure wave generation using the methods of characteristics, Heinz Struck, MSFC; (4) modified Broadwell/Tsu model of SRM igniter pulse and overpressure wave generation, Mark Silita, Thiokol; and (5) blast wave theory of overpressure wave characteristics, Dr. Bob Ried and Carl Scott, JSC. A brief discussion of methods (2), (3), and (5) can be found in Appendices A, B, and C, respectively. These three theories and others not discussed have limitations; however, they do add understanding to the overpressure phenomenon and provide good scaling relationships. The modified Broadwell/Tsu and the blast theory approaches provide reasonable estimates of the STS-1 levels. The data spread of the 6.4 percent model is quite large, as can be seen from Figure 25 (Section IV), and is believed to encompass all the expected launch values. This data variability is inherent in the ignition overpressure phenomenon and its transient

characteristics, and is due in large part to the extreme sensitivity of the resulting overpressure wave to the initial start-up characteristics of the motor. This variability is not only evident in the 6.4 percent model data but also full-scale Titan data, as well as other model tests that have been conducted in the past.

SECTION II. STS-2 SOLUTION APPROACHES

Unless some means could be achieved to suppress the overpressure environment, it was clear that the STS-2 Shuttle could not be launched without undue risks. Three basic conceptual approaches were open as means for suppression: (1) to attack the source of the overpressure and thus reduce its levels, (2) to contain the overpressure within the ML so that it does not reach the Shuttle vehicle, and (3) to relieve the pressure beneath the ML by opening up the sides of the enclosed volumes. Consideration of each of these approaches, however, had to be tempered by various other systems constraints: (1) there must be no slippage in the STS-2 launch date; (2) all covers used for containment must be either removed or burned away before the vehicle rose above the MLP in order to meet the acoustical environments; (3) aspiration requirements and negative delta pressures on the MLP must stay within design limits; (4) water quantities available for acoustic suppression were the upper limit of water available for overpressure suppression (in other words, water could only be diverted or rerouted, no new source available); (5) liftoff clearance envelopes could not be exceeded; (6) debris must be contained; (7) thermal environments could not be increased; and (8) some type of side deflector under the ML must be present to protect facility equipment.

The preferred approach was to attack the source, which could have been done by changing the SRM chamber pressure rise rate or by secondary injection into the SRB plumes. Altering the SRM was not possible within the limited available schedule, in that, in all probability, it would have required two or three years and additional motor qualification firings to achieve a satisfactory conclusion.

The other approach within the same general category of killing the source would be the injection of water into the plume. As stated previously, this action would change the density, cool the flow, quench after-burning, slow down the accelerating mass particles, and act as a shield containing the wave within the MLP. This approach certainly appeared to be a viable option and was given prime consideration as a part of the overall STS-2 solution.

The second general approach area, that of containing the overpressure within the ML, also would produce a satisfactory result; however, within the constraints discussed previously, such an approach would certainly be burdensome. Because of the uncertainty of water injection scaling, however, it was added to the list of possible STS-2 solutions for redundancy or insurance. Considered containment devices were classified into two categories: (1) soft covers that disintegrate shortly after contact with the SRM plume and (2) hard covers, such as trap doors, that move out of the way of the plume after the overpressure wave has passed.

The third general approach, relieving the pressure beneath the ML to minimize the buildup in the pressure, was another suppression technique considered. Specifically, consideration was given to (1) complete removal of the side deflectors and (2) louvered side deflectors to reduce the blockage area. Complete removal of the deflectors was not effective. The separation of the SRB on the Space Shuttle is slightly larger than can be completely accepted by the exhaust trench; consequently, the exhaust impinges directly on top of the SRB exhaust trench, which was the reason for the side

deflectors in the first place. One model test firing with complete removal of the side deflectors showed an aggravated overpressure. The other approach, louvered deflectors, would deflect the SRB exhaust flow into the trench and, thus, allow the pressure to be relieved. These louvered deflectors did, in fact, relieve the overpressure. Unfortunately, the Tomahawk motor that was used in this test had an abnormally high P_c rise rate (approximately three times higher than average). The resulting adjusted overpressure levels were very low, and the overpressure community was reluctant to accept these results. It was decided, however, to pursue this approach at some later date. Table 2 summarizes the options considered.

TABLE 2. OVERPRESSURE SUPPRESSION OPTIONS CONSIDERED

Source Reduction
1. Water injection into SRB plume. 2. Change $\dot{P}_c$ of SRB. 3. Injecting foam or other materials. 4. Helium bags in ML and trench. 5. Remove flame bucket and deflectors.
Containment
1. Hard covers. a. Trap doors b. Baffles c. Shield between SRB and Orbiter. 2. Soft covers. a. Tarpaulin. b. Troughs filled with water c. Divider between SSME and SRB plumes. d. Water bar barriers (sausages) in SRB holes.
Relieving the Pressure
1. No side deflectors. 2. Louvered side deflectors.

In order to evaluate these options and arrive at an overall solution, a series of parametric tests and, subsequently, 6.4 percent model tests was run.

SECTION III. PARAMETRIC TESTS AND RESULTS

To effect general cost savings and schedule optimization, several parametric tests were run with an overpressure pulse generator, i.e., without hot-firing the 6.4 percent model.

One of these tests consisted of a simulation of the overpressure wave in conjunction with various containment devices. The simulation of the overpressure, engineered by Garland Johnston and Jess Jones (MSFC), consisted of a small steel chamber with a nozzle opening, a device referred to as a "popper." A pyrotechnic charge was set off in the chamber. The chamber and nozzle were sized to give the overpressure wave characteristics, amplitude, and frequency. By placing this "popper" device in the flame trench and firing it upwards, a typical overpressure environment could be created. Several firings a day, in conjunction with different containment devices, could be accomplished. This testing activity allowed sorting out various approaches quickly and cheaply. Table 3 lists the general containment devices studied and the results obtained.

TABLE 3. OVERPRESSURE CONTAINMENT DEVICES

Configuration	Suppression
1. SRB drift hole (secondary hole) cover (solid and flexible)	Little
2. Vertical wall between SSME and SRB plumes	Little
3. Combination of 1 and 2	Little to moderate
4. Cover around SRB exhaust hole (primary) and drift hole (secondary) (solid and flexible)	Significant
5. SRB primary hole cover	Moderate

In summary, these tests showed that:

1. Any type of cover that does not fail suppresses the waves.

2. The wave mainly comes up around the SRB side, not on the SSME side.

3. Covering the primary hole is more important than covering the drift hole (secondary hole).

4. Dividers between the SSME and SRB have little effect on Orbiter overpressure environment.

Another off-site supporting test was developed to address how water can act to reduce overpressure; i.e., how water can act as a barrier or shield to contain the overpressure wave within the ML. The off-line test setup as a means of quantifying the above effect consisted of a simulated overpressure wave and a vertical water wall and enabled thickness, droplet size, etc., to be varied.

The simulated overpressure wave was generated in two ways: the popper described previously and a special acoustical horn with a pulse output. Since the scale model frequency was a factor of 16 higher than full scale, the issue of water barrier effects as a function of frequency needed to be addressed. This could best be done by varying the waveform, i.e., pulse frequency. Thus, most of the data used were acquired using the special acoustical horn approach.

The results of the above testing can be summarized as follows:

1. A solid sheet of water as opposed to a homogenous droplet mixture is required to significantly suppress the wave. The thickness of the water sheet required for attenuation depends on the frequency of the wave.

2. Water spray of any practical thickness provides little attenuation of the wave.

The results of this study and the corresponding scaling parameters are shown in Figure 16, which plots the test results, showing transmission loss as a function of frequency and thickness. Also, shown for comparison is the limp wall data found in the literature. Applying these data to the full-scale Shuttle vehicle shows that a 7-in. solid sheet of water is required to block or attenuate the 6-Hz overpressure wave and reduce its energy level by a factor of four. A portion of these results was verified for the scale model in subsequent hot firings.

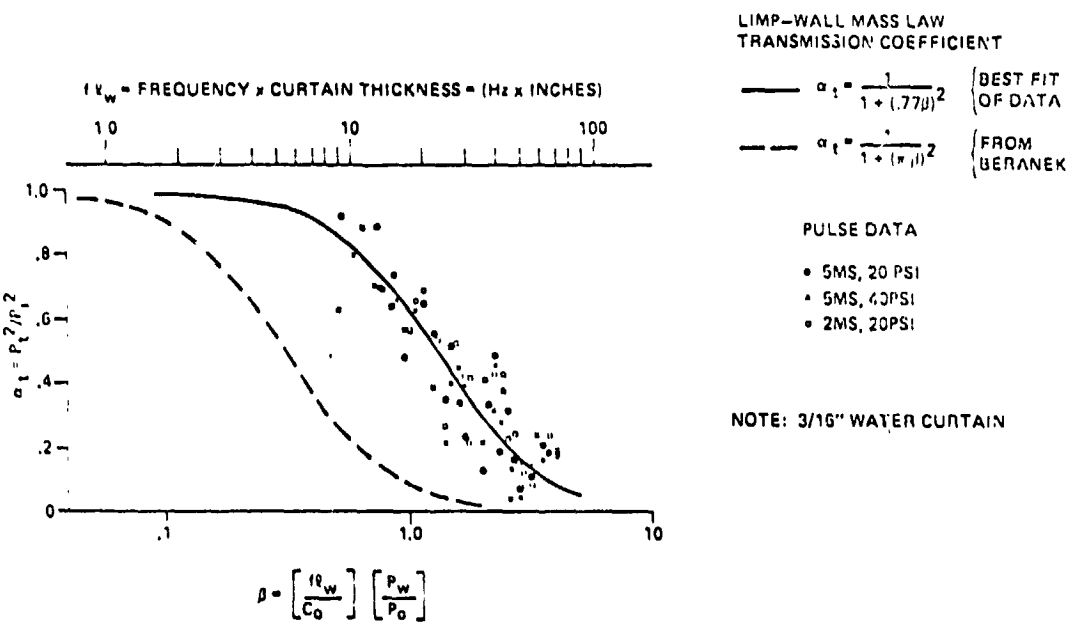

Figure 16. Transmission coefficient for a pulse incident on water curtain in air.

SECTION IV. 6.4 PERCENT SCALE MODEL TEST PROGRAM AND RESULTS

The scale model test program was conducted in two phases by MSFC test personnel, led by Jim Ralston. Phase I was a continuation of the parametric studies started off-line for preliminary evaluation of proposed fixes. Phase II was a detailed evaluation of the selected fixes and a determination of the overpressure environment to use for STS-2 loads verification. The instrumentation plans, test plans, and data summaries were documented by Rockwell.

A. Test Program Configuration/Schedule

Initially, two tests were run using the STS-1 ML configuration including simulated SSME firings. These tests were conducted to re-establish the 6.4 percent scale model's ability to predict the overpressure levels experienced on STS-1; since, as presented earlier (Fig. 4), it was determined that

the Tomahawk did not scale the Shuttle SRM chamber pressure rise rate. To check plume geometry effects, test 2 was run with a nozzle extension on the Tomahawk, while test 1 used the used the Tomahawk as designed. No significant difference was found in results from use of the nozzle extension; therefore, further use of the nozzle extension was abandoned. Problems were, however, encountered in these total systems tests: (1) Noise levels from SSME's were high enough to mask the overpressure characteristics on many sensors, and (2) inherent ignition lag times between the firing of the two Tomahawks were large enough to substantially reduce the overpressure environment. This lag was exaggerated by an order of magnitude over full scale caused by the difference between scale model and prototype time scales. As a result of these two problems, two changes were made to the test configuration. The decision was made to test without hot firing the SSME's since they did not contribute to the overpressure wave. The SSME plumes were simulated using solid cylinders in order to properly block the SSME holes. Also, the model was split in half with a large steel plate; and only one SRM was fired, thereby simulating via reflection the other motor ignition overpressure wave. The rationale for taking this approach was that the largest overpressure value would occur if both motors fired simultaneously and both waves reached the vehicle center with the same characteristics. The splitter plate would give the same effect. The use of the splitter plate and a single motor, half-model firing saved costly motors and allowed for the concentration of the limited available instrumentation. This was very important because the overpressures at any given vehicle station vary around the circumference of the vehicle, and the pressure difference across the vehicle drives the internal loads in the vehicle. Figures 17 and 18 show the splitter plate configuration from two viewpoints, the first looking in from the wing tip and the second looking in from the SRB side. In the second view, the splitter plate can be seen in the flame trench as well as on the vehicle.

Figure 17. Splitter plate configuration looking at wind tip.

ORIGINAL PAGE
BLACK AND WHITE PHOTOGRAPH

Figure 18. Splitter plate configuration looking in at SRB's.

Instrumentation was placed to obtain values for vehicle delta pressures, Orbiter thermal shield pressures, SRB thermal shield pressures, and pressure in the ML on both the SSME and SRB sides. Figures 19 and 20 show the basic instrumentation used. In special tests, some minor changes were made; however, the core set was maintained throughout all the tests. The total number of overpressure measurements per test was generally 50.

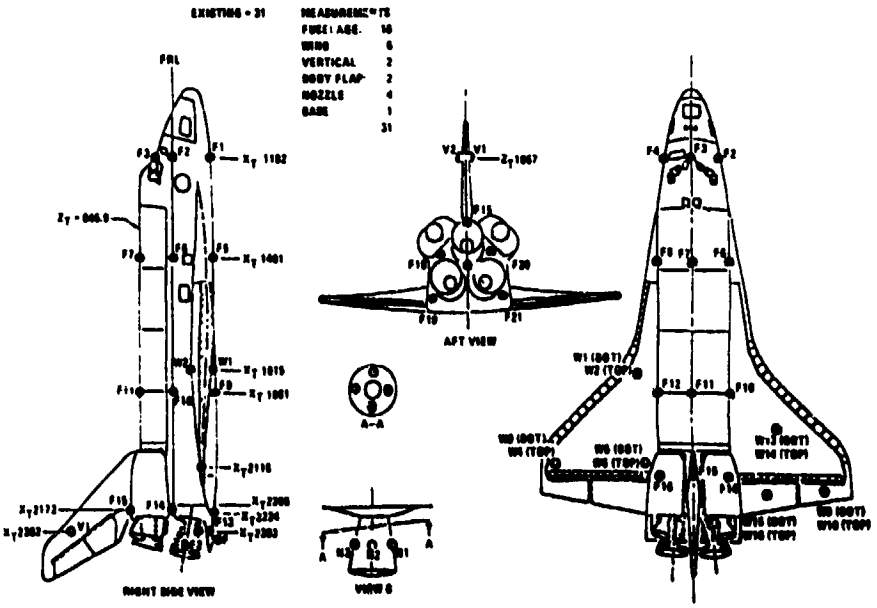

Figure 19. 6.4 percent overpressure instrumentation.

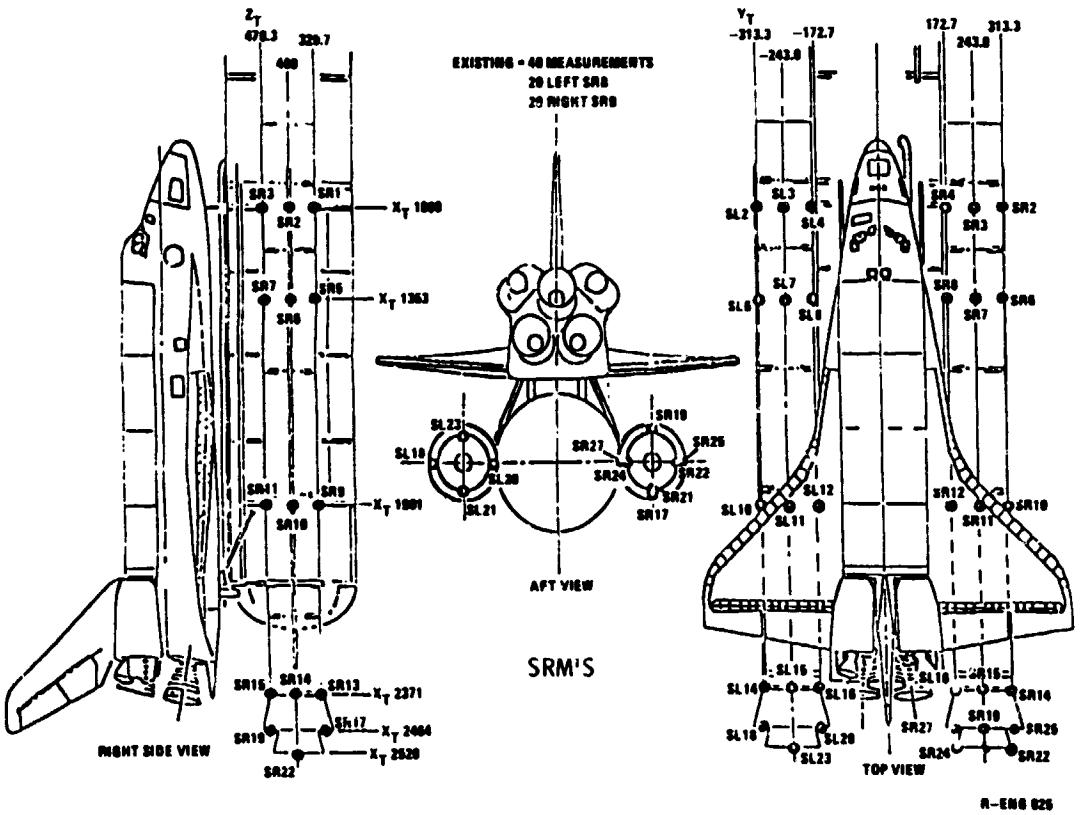

Figure 20. 6.4 percent overpressure instrumentation.

A matrix of all the tests run in the splitter plate configuration is shown in Table 4. Test fix configurations are shown versus test number with appropriate identifiers of each parameter indicated in the box. If no quantification was required, an X appears for each condition tested.

TABLE 4. 6.4 PERCENT MODEL SSV OVERPRESSURE TEST SUMMARY

SYSTEMS DYNAMICS LABORATORY/ED21	MARSHALL SPACE FLIGHT CENTER 6.4% MODEL SSV OVERPRESSURE TEST SUMMARY	GUEST OCTOBER 1981

SINGLE SRB TEST CONFIGURATIONS WITH FULL SPLITTER PLATE	TEST NUMBER
BASELINE (STS-1)	
SRB HOLE COVER PRIMARY	
SRB HOLE COVER SECONDARY	
DIVIDER WALL (FROM TOP DEFLECTOR TO BOTTOM HOLE)	
WATER INJECTION PRIMARY HOLE*	
WATER INJECTION SECONDARY HOLE*	
SRB SIDE PIPES (STS-1 FLOW)	
SRB SIDE DEFLECTOR	
SRB CREST WATER (STS-1 FLOW)	

NOTES: H = HARD COVER ON PLATE
E/S = COVER ON SOUTH EAST & WEST PART OF HOLE
WL = WATER LOCK
WT = WATER TROUGH
S = LIKE STS-1
L = LOUVERED DESIGN
N = NOZZLE EXTENSION
E = ELEVATED LOWEST 6 PIPE WITH HORIZONTAL FLOW
E/L = 60° DOWN FLOW
S = SSC = CREST WATER SYS DESIGN
N = SSC 3 NOZZLE INJECTOR DESIGN FOR STS 2
* = WATER IN THOUSANDS @ 0 FROM HORIZONTAL PER MANIFOLD NEAR SLP UNLESS NOTED OTHERWISE
** = SPLITTER PLATE ABOVE SLP REMOVED

PRIMARY — SECONDARY

PLAN B VIEW SRB HOLES IN SRB

B. Establishing Test Validity

To help establish the validity of the testing techniques, it is important to show that the scale model data did, indeed, represent the STS-1 environments. As was pointed out earlier, one key parameter in the overpressure phenomenon is the chamber pressure rise rate. If the scale model is representative of the full-scale environments, then the scaling theories presented earlier by Jones and Guest (MSFC) and Ried and Scott (JSC) should predict in a reasonable manner the STS-1 result, using the 0.4 percent baseline data. Indeed, this is the case. First, it is important to normalize the scale model data based on some function of $\dot{P}_c$. This is necessary since the Tomahawk motors have variability in $\dot{P}_c$ from firing to firing. It was shown in Figures 14 and 15 that the overpressure wave closely tracked the $\dot{P}_c$ in terms of shape and frequency. The same results follow for the scale model. The Tomahawk $\dot{P}_c$ has two distinct peaks with the first being the smallest. Since the first peak predominates in the $\dot{P}_c$ of the full-scale SRM and since the time lag of the second peak of the scale model removes it from importance in the liftoff sequence, only the first positive and negative peaks were analyzed. Figure 21 contains plots of the P_c and $\dot{P}_c$ of the Tomahawk, and Figure 22 is a typical overpressure wave. The amplitude and period of oscillation clearly track the $\dot{P}_c$; however, the second $\dot{P}_c$ spike is as large or larger than the first and clearly causes a second positive peak different from the full-scale results. This led to data evaluation problems which were resolved by reading only the first peak. As an additional correlation, the pressure on each Shuttle and facility element for each test was averaged and plotted as unnormalized pressure versus $\dot{P}_c$. Figure 23 is a plot of these values for tests 19, 20, 22, 27, and 28. Although there is some scatter in the data, they fairly well follow a linear trend.

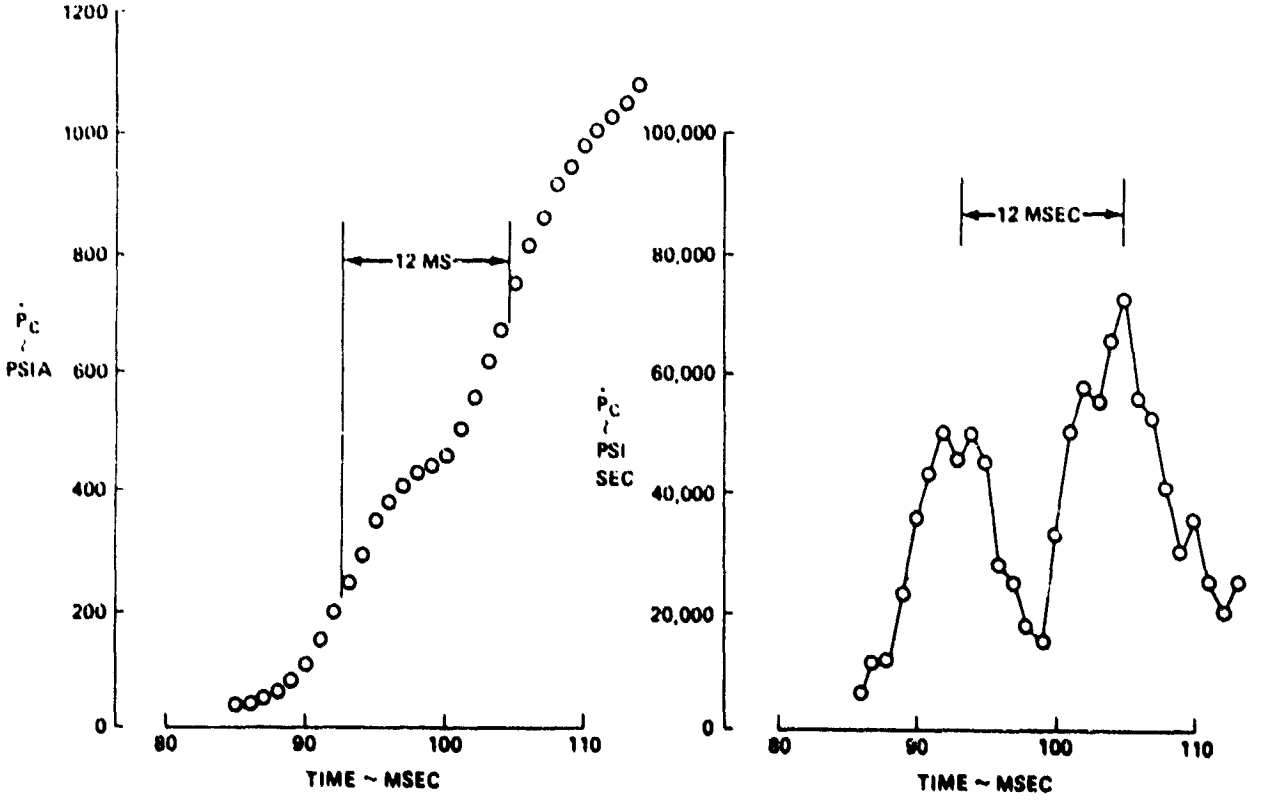

Figure 21. P_c and $\dot{P}_c$ rise rate history.

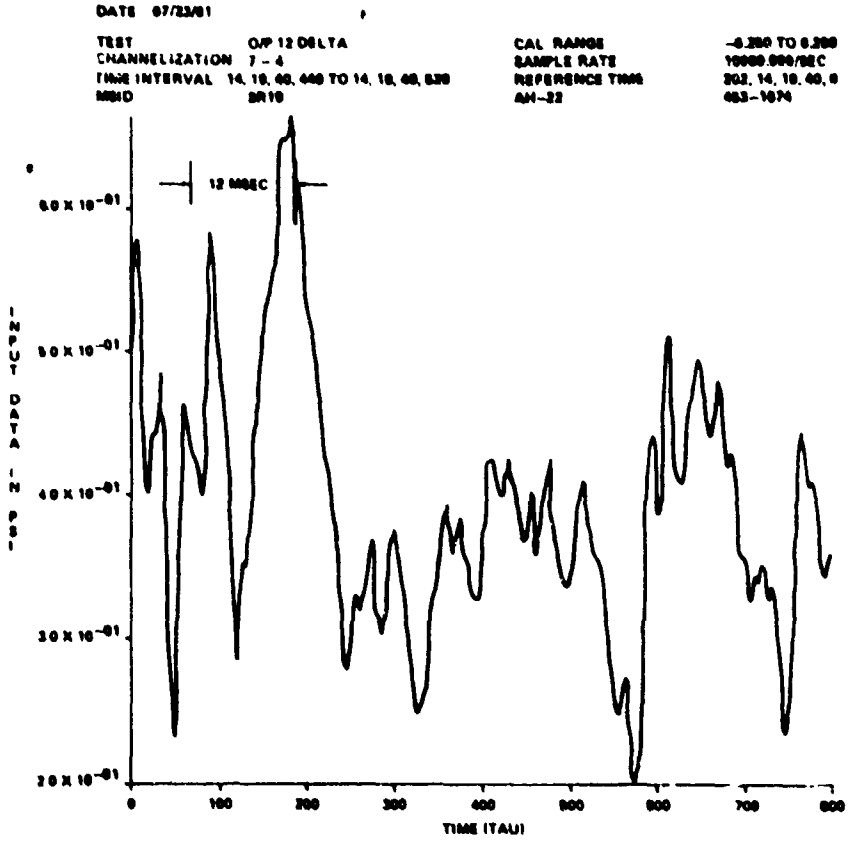

Figure 22. 6.4 percent scale model typical overpressure wave.

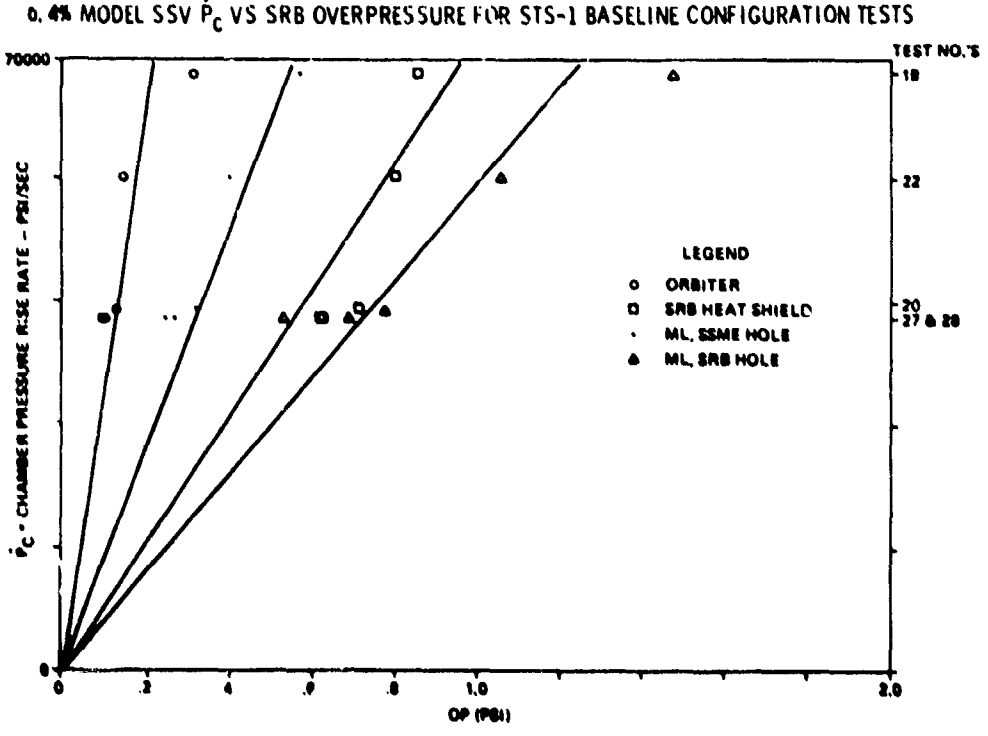

Figure 23. Baseline overpressure scaling with P_c.

Typical test results with the STS-2 fix configuration show the same trend. Results for tests 24, 25, and 26 are shown on Figure 24.

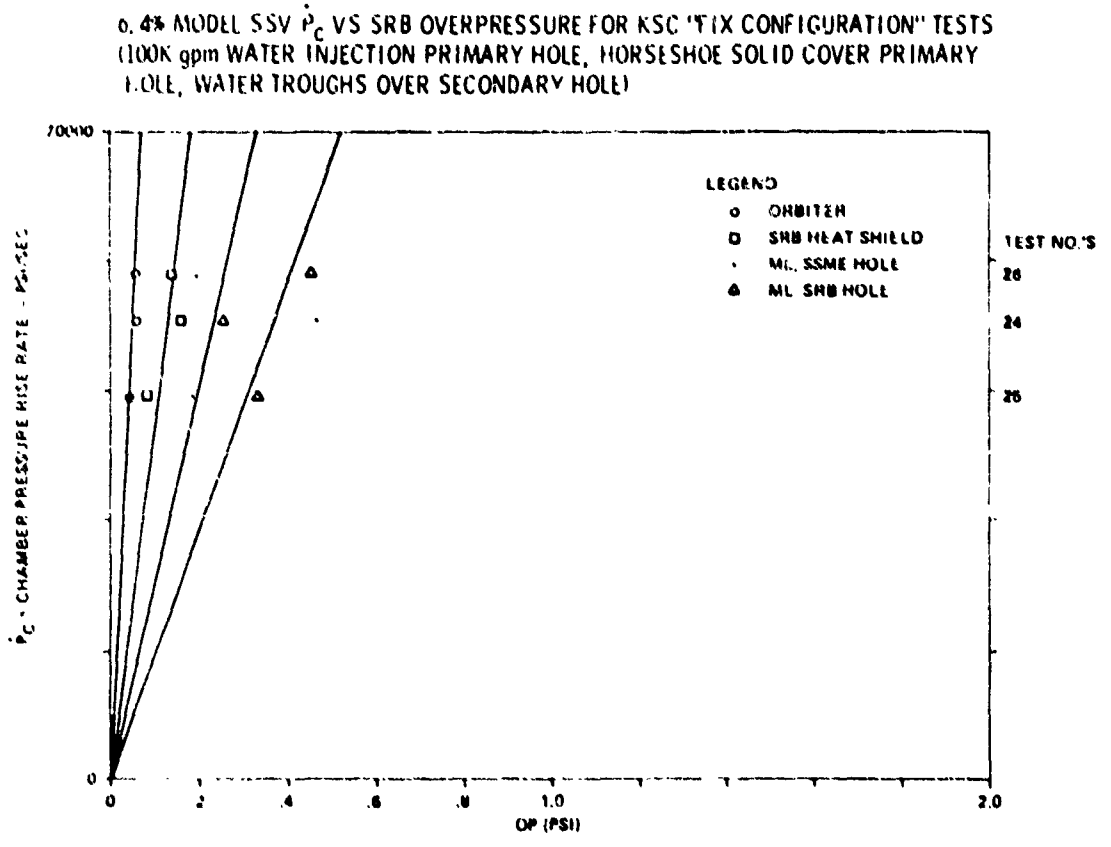

Figure 24. STS-2 fix overpressure scaling with $\dot{P}_c$.

The proof of the approach being used is whether this scaling approach duplicates the STS-1 results. Pre-STS-1 predictions were shown in Figure 4, based on very limited data. Using the results of the present scale model data for the splitter plate configuration provides equally good results. Figure 25 shows peak amplitudes scaled linearly to $\dot{P}_c$ plotted versus vehicle station. Superimposed are the STS-1 values. The curved line is the typical decay curve of a weak shock versus distance given as a reference point.

The band is the spread in the scale model data. A good fit is obtained, except for two measurements; one of which can be easily explained. This measurement, located against the splitter plate, shows reflected amplification producing values too large. The other exception is the Orbiter thermal shield, which is under-predicted using the Jones and Guest linear scaling law. Sam Doughtery of Rockwell International showed that these measurements followed a $\dot{P}_c^2$ scaling law (Fig. 26).

Reid and Scott, using iso-intropic gas dynamics theory, showed that a scaling of $\Delta P/R \sim A_e \sqrt{hc/a_\infty^2}\ (P_c)^2/\overline{P_c}$ does an improved job of describing the data. They first plotted the pressure data as a function of distance from the source showing a fairly good correlation with 1/R (distance).

Figure 27 is a plot of these data for STS-1, while Figure 28 is the same plot for scale model test 19. STS-1 data are shown as a dotted line on Figure 28

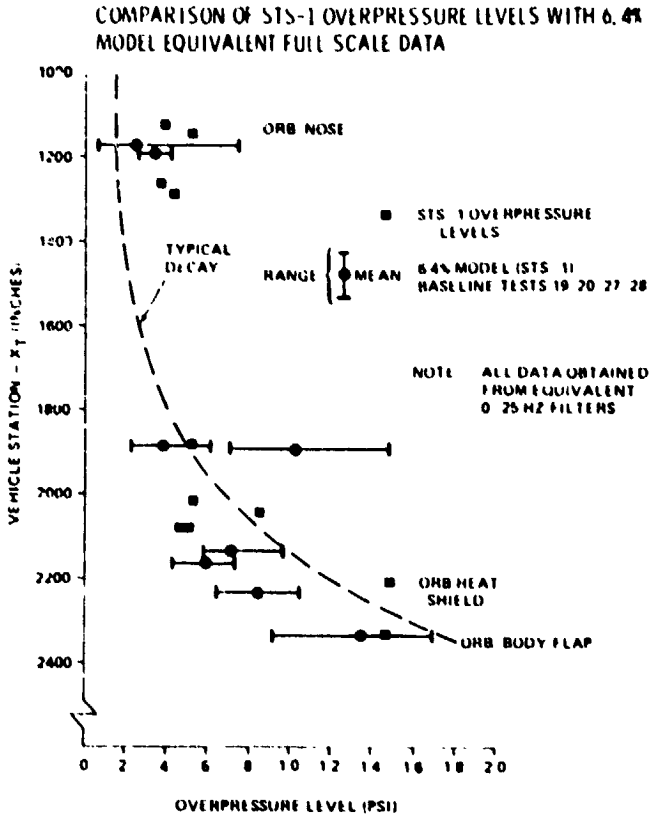

Figure 25. Scale model versus STS-1 overpressure.

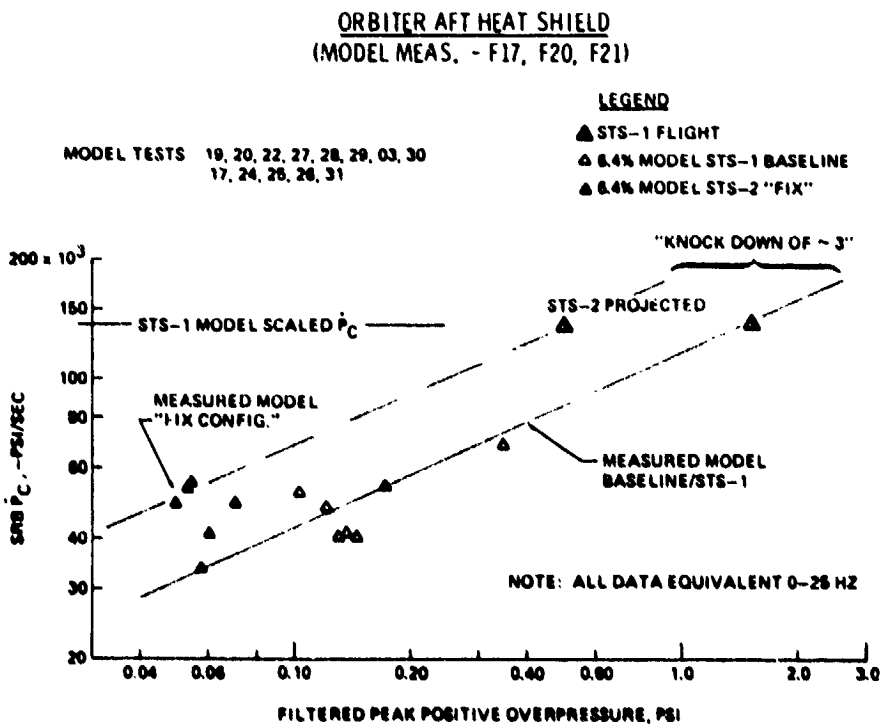

Figure 26. Orbiter thermal curtain scaling.

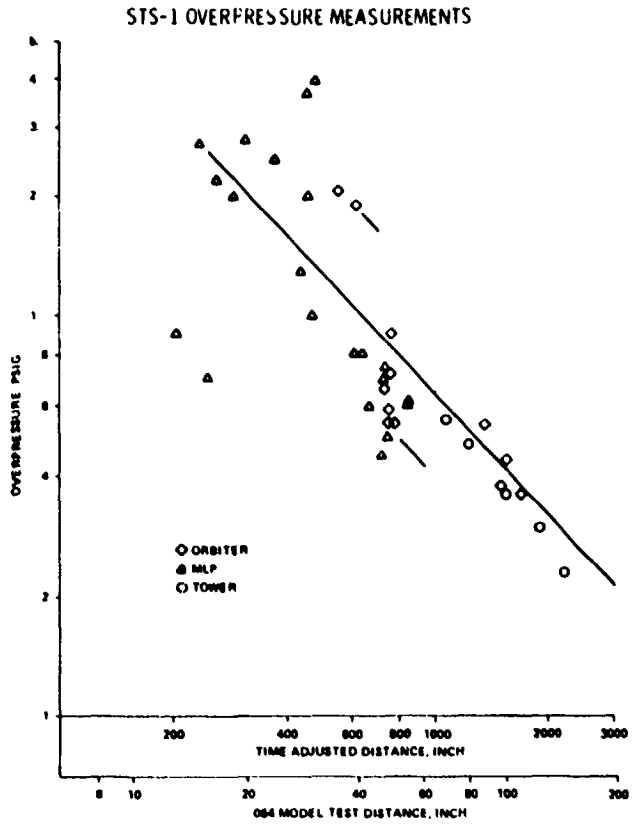

Figure 27. STS-1 overpressure versus distance.

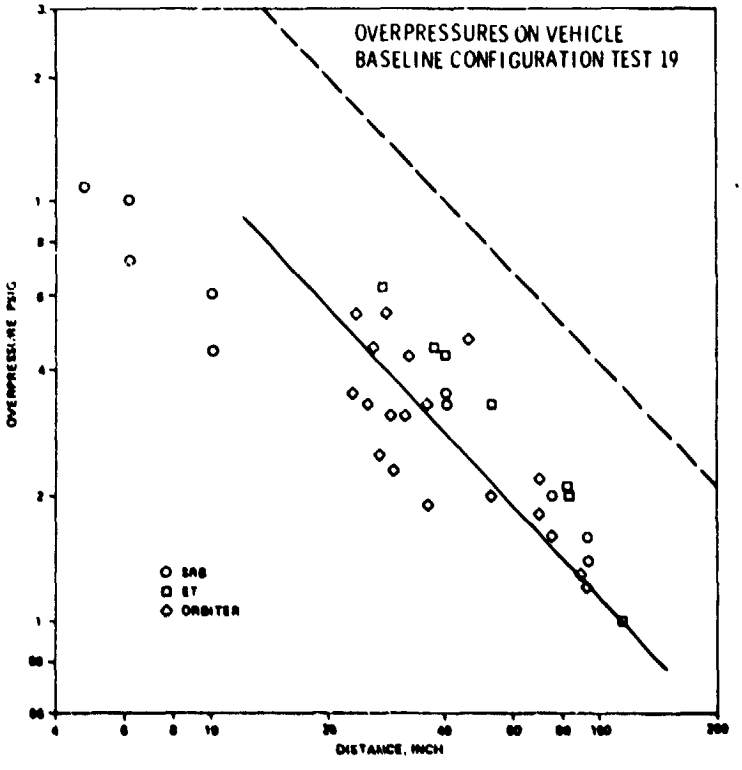

Figure 28. Scale model test 19 overpressure versus distance.

This correlation allowed them to go to the mentioned scaling law, which produced the results in non-dimensional form shown in Figure 29.

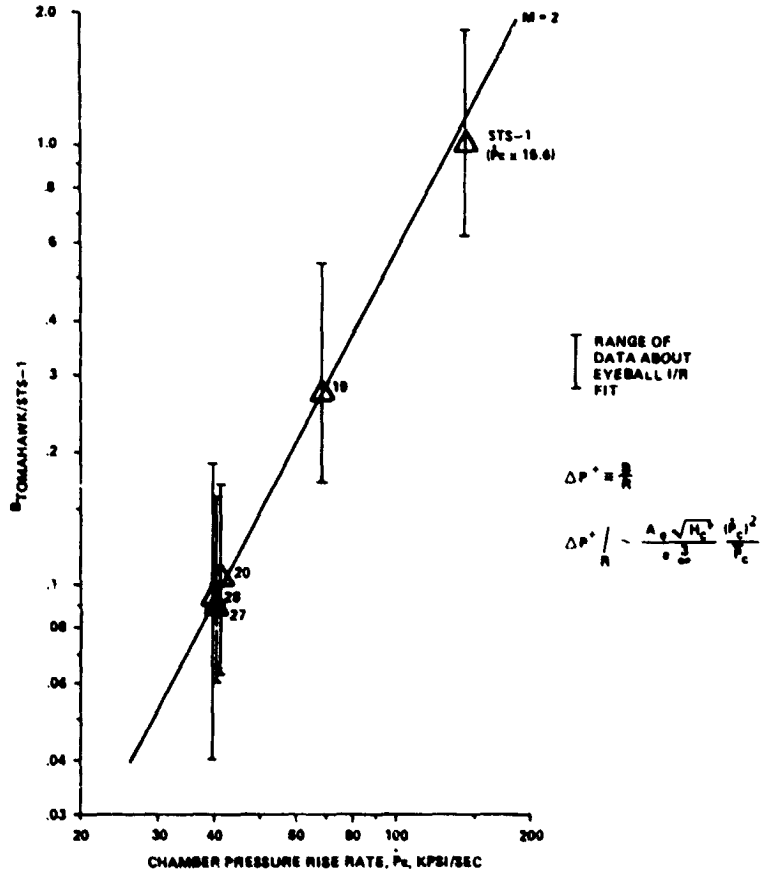

Figure 29. Overpressure versus $\dot{P}_C$.

A good correlation exists using this theory for extrapolating scale model data to STS-1. This approach, applied to the Orbiter measurements, predicts results similar to those of Jones and Guest. Using the Broadwell and Tsu model, which is linear in relationship, the nonlinear aspects of Ried's model give an overall better fit of the data than the linear models; in that, the data spreads are less than the linear approaches.

These two independent approaches, although not giving identical results, clearly establish the ability of the scale model to predict full-scale results without water injection.

C. Test Evaluation Techniques

Data from the 6.4 percent scale m[illegible] test program were analyzed and evaluated in several ways. First, it was desirable to get a quick assessment of the relative merits of fixes so that decisions could be made for the next test. MSFC recommended that this be accomplished by grouping the

measurements, such as Orbiter, Orbiter thermal shield, etc., and averaging the peak pressure measurements. To account for the variation in $\dot{P}_c$ between different motors, the data were normalized to an average $\dot{P}_c$ before the grouping and averaging process. This average $\dot{P}_c$ is 45,625 psi/sec and was obtained from the average of the initial series of tests when this procedure was established. Ratios were then determined by dividing the average data for an individual test by the average data for the baseline test. Originally, test 5 was used for this baseline. Later, tests 19 and 20 were used. The final assessment used tests 19, 20, 27, and 28 for pitch plane data, and tests 29 and 30 for the yaw plane data. Table 5 summarizes the procedure.

TABLE 5. QUICK-LOOK DATA EVALUATION PROCEDURE

1. Read first positive overpressure peak. Second positive peak of Tomahawk not applicable to Shuttle SRM's (Reference Figs. 14 and 21).

2. Determine maximum $\dot{P}_c$ of first pressure chamber peak rise rate.

3. Normalize peak pressures by ratio of individual peak chamber pressure rise rate to average of Tomahawk (45,625 psi/sec).

$$p_1^+ \left(\frac{45{,}625}{\dot{P}_{c_1} \text{ (Indices)}} \right) = p^+ \text{ (normalized)}$$

4. Compute the ratio of normalized pressure (per measurement) between individual test and the average baseline tests (per measurement).

$$\text{Ratio} = \frac{\text{Normalized pressure (per measurement) for individual test)}}{\text{Average normalized pressure (per measurement) baseline test}}$$

Ratio is reduction of fix relative to STS-1 hardware.

5. Average the normalized pressure ratioed data by groups: SRB thermal heat shield, vehicle/Orbiter, MLP SRB side, MLP SSME side, Orbiter thermal shield.

These ratios of the average pressures of scale model tests are summarized in Tables 6 and 7. These tests and test configurations are identical with those shown previously in Table 4.

As an additional evaluation technique, Rockwell International/Space Division took the individual pressure measurements as a function of time and calculated delta pressures as a function of time by taking differences between all matched pairs of instruments on each side of the vehicle. These peak delta pressures were then ratioed to the baseline (STS-1) delta pressures. These ratios were used to multiply the STS 1 flight measured forcing functions. All data were first normalized to $\dot{P}_c$, as discussed previously, to remove $\dot{P}_c$ scatter in the data. Rockwell first used a linear $\dot{P}_c$ normalization. The final data used the Ried and Scott $(\dot{P}_c)^2/\overline{P}_c$ normalization. The ΔP forcing function determined in this fashion was multiplied by an appropriate data scatter factor and applied to the Shuttle dynamic model to generate loads. Since the STS-2 fixes shifted the basic overpressure wave frequency but not the general character, a correlation to STS-1 ratio environment had to incorporate a frequency correlation also. This was accomplished by incorporating a frequency spread on the data.

TABLE 6. PRESSURE AMPLITUDE RATIOS

-----AMPLITUDE CORRECTION FACTORS-----

TEST	DESCRIPTION	VEHICLE ORBITER TANK	THERMAL CURTAIN SR19	THERMAL CURTAIN SR17	MLP SRB SIDE	SSME HOLE	ORBITER HEAT SHIELD
5	BASELINE	1.593	1.231	0.000	1.319	1 016	1.681
6	HCP, HCS, HD	0.201	2.519	0 000	1.876	0.102	0 211
7	HCS, HD	0.777	1 381	0 000	1.865	0.322	0.809
8	HD, WLP, WLS	0.530	0.737	0 000	3.591	0 285	0.492
9	HCP, HCS	0.295	0.278	0.000	1 770	0 921	0 365
10	WI, 40KP/30KS	0.256	0 266	0 000	1.123	0.478	0 228
11	WI, 40KP/30KS, -SD	0.355	0.215	0 000	1.240	0 700	0.421
12	WI, 70KP	0.265	0 443	0.000	1 007	0.749	0.190
13	WI, 70KP, WLS	0 413	0 092	0 000	1.631	0 543	0 113
14	WI, 70KP, HD	0 243	0 132	0.000	1 265	0.380	0.104
15	WI, 70KP, CWI	0.481	0 222	0.000	1 046	0 937	0 468
16	WI, 70KP LSD	0 079	0.011	0.240	0.245	0.168	0 138
17	WI, 70KP HCP, WLS	0 241	0 184	0.202	1 398	0 865	0 259
18	WI, 70KP, H/SCP	0 305	0 367	0.329	0 788	0 650	0 226
19	BASELINE	1 375	1 252	1.561	1.264	1 121	1 233
20	BASELINE	1.005	1 240	1.165	1 059	1.062	1.053
21	WI, 105KP	0 460	0 526	0.590	0.645	0 537	0.564
22	BASELINE,-NOZZ, EXT.	0.847	1 267	0.910	1.010	1 007	0 907

BASELINE USED CONSISTS OF
TEST #19, TEST #20, TEST #27, TEST #28

Ref.Pc RATE = 45625 (psi/sec)

TABLE 7. PRESSURE AMPLITUDE RATIOS

-----AMPLITUDE CORRECTION FACTORS-----

TEST	DESCRIPTION	VEHICLE ORBITER TANK	THERMAL CURTAIN SR19	THERMAL CURTAIN SR17	MLP SRB SIDE	SSME HOLE	ORBITER HEAT SHIELD
23	HCP, WTS	0 744	0.632	0.778	1.181	0.850	0.402
24	WI, 100KP, WTS, HCP	0.357	0.579	0.173	0.388	1 313	0 415
25	REPEAT 24	0.310	0.260	0.337	0.529	0 651	0.434
26	REPEAT 24	0.305	0.438	0.354	0.489	0.486	0.282
27	REPEAT 19 (BASELINE)	0.834	0 739	0.584	0.724	0.851	0.952
28	REPEAT 19 (BASELINE)	0.787	0 769	0.690	0 954	0.965	0.762
29	BASELINE, -UPPER SP	0.854	1.540	1.450	1.354	0.851	0.747
30	REPEAT 29	0 641	0 864	1.082	0.995	0.744	0.488
31	KSC FIX NO UPPER SP	0.299	0.176	0.276	0.784	0.472	0.330
32	REPEAT 31	0 216	0.089	0.320	0.896	0.171	0.096
33	REPEAT 31	0.145	0 260	0.275	0 591	0.514	0 253
34	REPEAT 23	0.761	0.647	0 841	1.202	0.953	0.623
35	WI, 100KP	0.451	0 226	0.587	0.643	0.872	0.324
36	100K WI, SCP/S	0.292	0.152	0.091	0 473	0.666	0 273
37	REPEAT 36	0.321	0 111	0 397	0.755	1.019	0.356
38	WTP,WTS	0.435	0.688	0.395	0.958	1.177	0.591

BASELINE USED CONSISTS OF
TEST #19, TEST #20, TEST #27, TEST #28

Ref.Pc RATE = 45625 (psi/sec)

All the data were processed by MSFC with some evaluation and analysis performed by Rockwell International/Space Division. This system is summarized in Table 8.

TABLE 8. APPROACH FOR DETERMINING OVERPRESSURE ENVIRONMENTS

1. Time response of each individual pressure measurement digitized.
2. Individual time response normalized to $\dot{P}_c$.
3. Delta pressures determined by taking differences of matched pairs of instruments.
4. Peak delta pressures are read, first positive and negative peaks.
5. Ratios of peaks to baseline peaks are determined.
6. STS-1 environment multiplied by these ratios to get nominal STS-2 environment.
7. Frequency differences between STS-1 environment and STS-2 fix data were determined and used as a spread in the forcing function data.
8. Forcing function data multiplied by data scatter factor.
9. Loads run for Shuttle system using these environments.

To insure that this approach was valid, Rockwell/Space Division ran a simulation of the STS-1 response using the STS-1 overpressure environment and other key vehicle parameters. A good match was obtained by going to a detailed Orbiter shell model and using 200 vehicle system modes. With this validation of the model, the different fixes and the final verification of STS-2 vehicle could be assessed. Tables 9 and 10 are a partial listing of the delta pressures and load ratios obtained by Rockwell.

D. Phase I Testing

Tests 3 through 18 (Table 4) were the Phase I parametric tests used for selecting the preliminary STS-2 fix configuration. Of these, tests 3, 4, and 5 represented the STS-1 baseline used as a reference. In these Phase I parametric tests, models of the fixes were not high-fidelity representations of the actual KSC implementations of the fixes, because, in part, KSC designs were still in progress. Tests 6 through 18 tested various generic suppression techniques. Tests 6 through 9 were to evaluate covers and covers with a hard divider between the SSME and SRB plume. Covers give good reduction in the Orbiter; however, the levels within the MLP are increased. These covers were 1/4-in. steel plates bolted to the top of the MLP. The presence of the hard divider had little or no effect on Orbiter overpressure data. Tests 10 through 18 evaluated the effects of water injection in conjunction with various hard and soft cover concepts. Water reduces all levels and also reduces the data spreads. Adding covers with water had little effect in comparison with water alone. Tests 11 and 16 were run in this series to evaluate the effects of the SRB flame trench side deflector. Test 11 had the side deflector removed. In this case, the overpressure wave reflected off the top of the trench and increased the level. Test 16 had a slotted side deflector which reduced the levels significantly; however, the Tomahawk $\dot{P}_c$ was excessively high, and the over-normalization renders the results questionable. Even with the assumption of a reduced $\dot{P}_c$, the slotted side deflector offers some potential for reducing overpressure. Test 15 was run to check the hypothesis that the crest water reflected the overpressure wave, thus increasing the magnitude. The crest water was changed from a horizontal flow to 30 degrees down, which was found to increase the levels, indicating that the crest water configuration on STS-1 decreased the level instead of increasing it as hypothesized.

TABLE 9. EQUIVALENT FULL-SCALE SRB IGNITION OVERPRESSURE

DATA CORRECTED FOR P_C VARIATIONS
BASELINE TEST: P075–019

TEST NO. & DESCRIPTION P075 – / MOD'S FROM B/L		DIFFERENTIAL OVERPRESSURE					OVERPRESSURE		SRB SKIRT RATIO	$\dot{P}_C$	$\frac{\dot{P}_{C-19}}{\dot{P}_{C\,XX}}$
		FWD. FUSEL.	MID. FUSEL.	WING C. P.	I'BD ELEV.	O'BD ELEV.	ORB BASE	ET BASE			
005		.219 –.196	.662 –2.17	.486 –1.89	.818 –2.65	.913 –1.74	3.29 –3.14		1.42	35K	1.8
006	HARD COVER P&S HARD DIVIDER										
007	HARD COVER SECONDARY HARD DIVIDER										
008	H_2O LOGS P&S HARD DIVIDER										
009	HARD COVER P&S	.100 –.070	.284 –.701	.157 –.496	.306 –1.04	.255 –.508	.708 –.899		1.85	70K	1.3
010	40K GPM P 30K GPM S										
011	40K GPM P 30K GPM S	.079 –.081	.466 –1.08	.387 –.925	.597 –1.20	.608 –.969	1.80 –1.71		.615	52.5K	1.2
012	70K GPM P	.088 –.095	.238 –1.09	.195 –.789	.205 –.923	.344 –.569	.909 –.868		.374	50K	1.3
013	70K GPM P H_2O LOGS S	.050 –.050	.278 –.920	.124 –.536	.215 –.659	.175 –.385	.670 –.646		.776	47.5K	1.4
014	70K GPM P HARD DIVIDER	.118 –.106	.600 –2.34	.378 –1.49	.617 –1.75	.536 –.941	.473 –.439		1.09	47.5K	1.3
015	70K GPM P CREST WATER ANGLE CHANGE	.161 –.184	.682 –2.84	.496 –1.71	.849 –2.55	.493 –1.39	1.46 –1.38		.818	35K	1.8
016	70K GPM P LOUVERED SIDE DEFL.	.030 –.050	.137 –.767	.096 –.485	.189 –.534	.199 –.368	.478 –.452		.448	127.5K	0.5
017	70K GPM & HARD COVER P. WATER COV'S S	.086 –.058	.138 –.794	.143 –.394	.167 –.629	.186 –.590	.648 –.619		.222	55K	1.2
018	70K GPM HARD COVER	.140	.792	.596	.800	.701	1.508				
019		.260 –.261	.700 –1.58	0 –1.04	.341 –1.09	.502 –.800	2.10 –2.00		.998	66K	1.0
020		.291 –.454	1.37 –3.90	1.01 –4.53	1.98 –6.29	1.41 –3.01	4.62 –4.40		1.64	42.5K	1.6
021	105K GPM P	.118 –.050	.348 –.687	.213 –.698	.322 –.902	.296 –.556	.773 –.737		.339	47.5K	1.4
022	BASELINE NOZZ EXT	.287 –.165	.716 –2.13	.574 –2.35	.446 –2.40	.348 –1.15	1.09 –1.04		1.03	51K	1.3
023	HARD COVER P WATER TROUGH S	.071 –.074	.238 –.317	.274 –.777	.224 –.659	.140 –.406	1.15 –1.14		.306	50K	1.3
024	100K GPM HARD COVER P WATER TROUGH S	.107 –.084	.323 –.546	.242 –.874	.414 –1.03	.288 –.508	.657 –.624		.248	50K	1.3
025	REPEAT – 024	.085 –.076	.279 –.688				.658 –.635		.215	45K	1.3
026	REPEAT – 024	.058 –.065	.162 –.667	.396 –1.39	.189 –.584	.250 –1.17	.648 –.619		.162	61K	1.1
027	REPEAT – 019	.591 –.464	1.17 –2.46	.806 –1.70	.955 –2.00	.335 –1.01	2.19 –2.08		.657	40K	1.7

TABLE 10. SKB IGNITION OVERPRESSURE EQUIVALENT FULL SCALE FORCING FUNCTION

TEST NO.	DESCRIPTION	DIFFERENTIAL OVERPRESSURE (Z DIRECTION)					OVERPRESSURE (X DIRECTION)		SRB SKIRT RATIO
		FWD FUSE.	MID FUSE.	WING C.P.	I'BD ELEV.	O'BD ELEV.	ORB BASE H/S	ET BASE	
STS-1	FLIGHT DATA	.26 -.26	.70 -1.58	.52 -1.04	.84 -1.69	.50 -.60	2.10 -2.00	.52 -.49	1.00
17	OPTIMUM MOD 70KGPM, HCP, WLS	.05 -.05	.13 -.72	.13 -.36	.17 -.57	.24 -.42	.59 -.56	.15 -.14	.28
24 THRU 26	PRELIM. KSC MOD 100KGPM, HCP, WTS	.07 -.07	.20 -.45	.13 -.26	.21 -.42	.13 -.15	.70 -.67	.17 -.16	.29
37	FINAL KSC MOD 100KGPM, WTP, WTS	.08 -.06	.14 -.44	.12 -.25	.17 -.40	.12 -.15	.77 -.74	.18 -.17	**

* NOMINAL PRESSURES IN PSI - UNCERTAINTY NOT INCLUDED

** QUESTIONABLE DATA

E. Preliminary Fix Selection

At the completion of Phase I of testing (through test 18), selection of water injection as a primary fix was made. In addition, a secondary fix consisting of hard covers for the primary hole and soft covers for the secondary hole was added as insurance because of the uncertainties of scaling factors for the water fix. However during the course of Phase II testing, the use of hard covers in the primary hole was discarded; and soft covers like those used in the secondary hole were installed instead. This change was made in response to an analysis by Dr. Terry Greenwood (MSFC) who found that, at liftoff, the SRB plume would impinge on the hard covers and be reflected back on the SRB heat shield, creating loads and thermal environments above the SRB thermal curtain capability.

The selected primary fix, water injection, was proposed by Guest and Jones based on their work in acoustical noise suppression. The design and implementation were accomplished at KSC. Figure 30 shows this water system (Fig. 30a is the scale model, whereas Fig. 30b shows the full scale configuration) which injects 100,000 gpm of water into each SRB plume primary hole. Eight nozzles are used: two producing 24,000 gpm of water each, on the north side of the haunches; two on the east side and two on the west side producing 12,000 gpm of water each; and two on the south side producing 2,000 gpm of water each.

The soft cover concept, based on the off-line tests conceived and run by MSFC, was originated by Dr. Max Faget (JSC), who showed that seven or more inches of water would contain the over-pressure wave. The concept is a series of troughs made of Kevlar and nylon filled with water to a depth of approximately 15 in. An individual trough is shown in Figure 31.

Figure 30a. 6.4 percent model SRB water injection system (KSC type) (scale model).

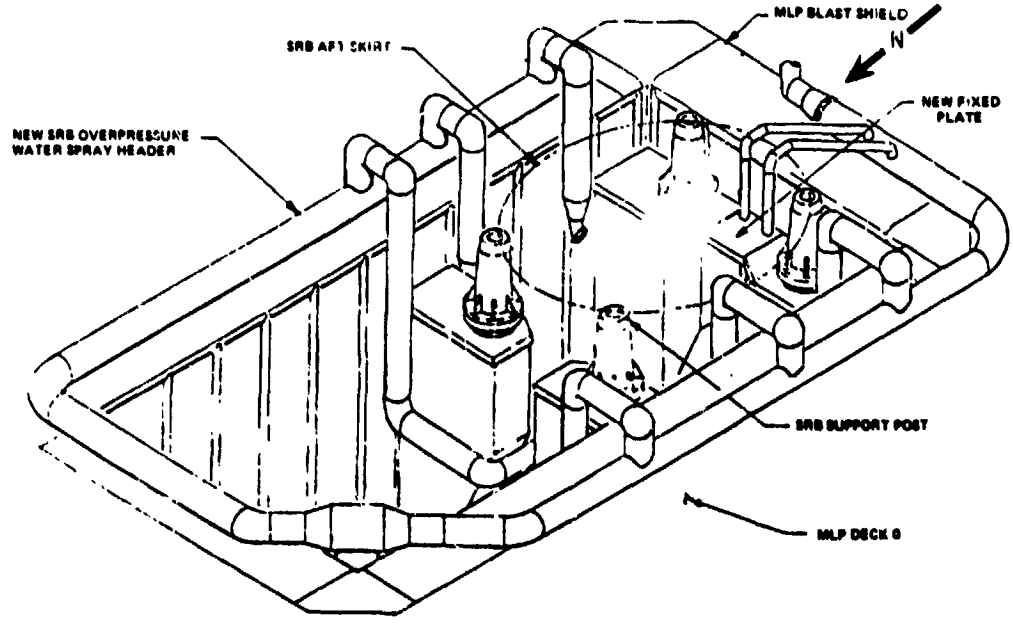

Figure 30b. 6.4 percent model SRM water injection system (KSC type) (full scale).

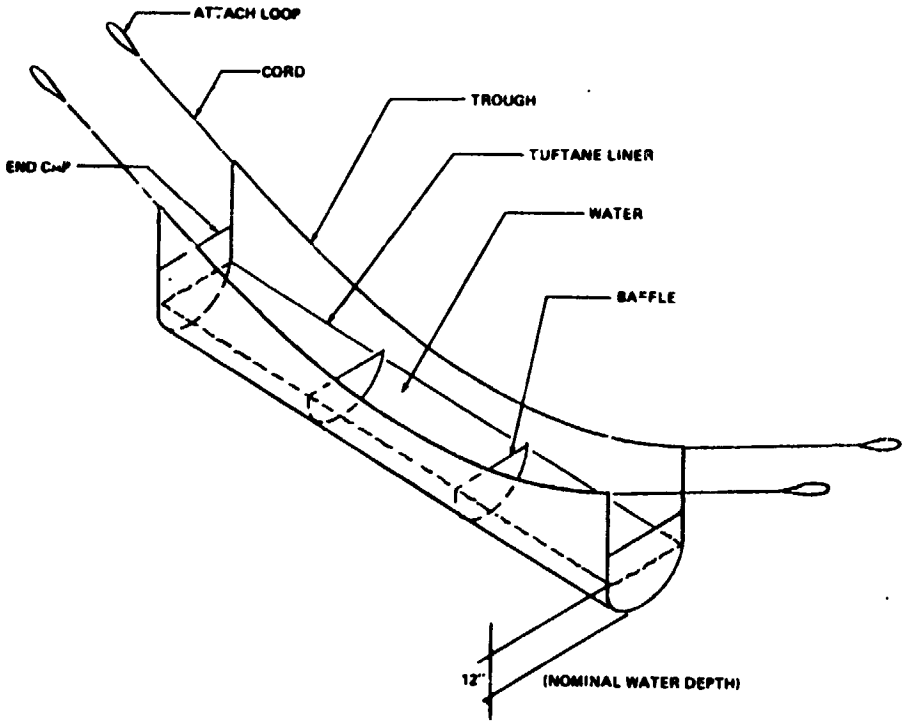

Figure 31. Typical water trough.

The main concern with water trough soft covers has been the debris issue. Vince Verderaime, Doug Lamb, and Denny Kross of MSFC; Bob Ried of JSC; and others did detailed dynamic and thermal analyses and failure analysis to show that a low risk debris condition existed.

The complete installation of the water troughs and water injection system is shown in Figures 32a and 32b, a picture of the scale model implementation of the concept and a drawing of the full-scale hardware, respectively.

Figure 32a. STS-1 fix configuration (6.4 percent model) (scale model).

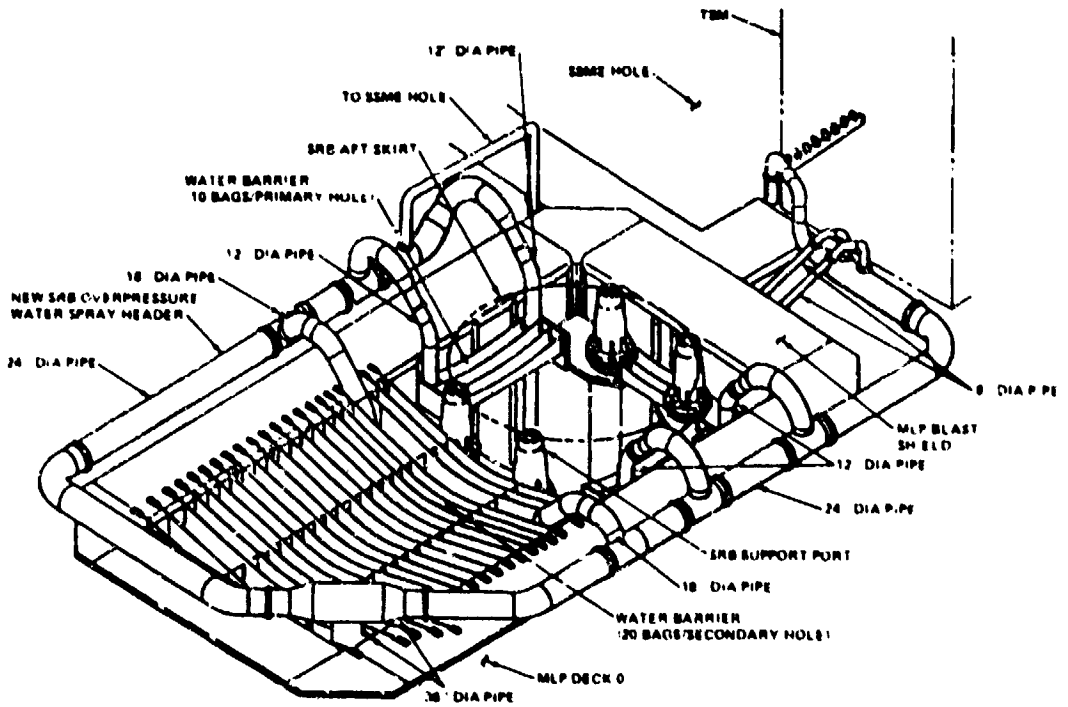

Figure 32b. STS-1 fix configuration (0.4 percent model) (full scale).

F. Phase II Testing

While the KSC-designed water injection system was being fabricated, the total model, including facilities, was refurbished to duplicate the STS-1 vehicle and launch pad configuration. During this activity, one discrepancy was found in the facility model. The flame deflector crest water in the scale model was on top of the divider; while in the actual KSC configuration, it was buried in the flame deflector crest. This condition required lowering the model crest water injection point approximately 3 in. to match full scale.

Instead of directly scaling the 0.4 percent overpressure environments to full scale, it was decided to develop a scale model ratio between the STS-1 baseline configuration and the fix configuration and apply this ratio to the STS-1 measured environments to establish STS-2 predicted environments. These STS-1 ratioed full-scale environments would then be used as the forcing functions for verification of the STS-2 loads and responses. This required that a good statistical sample of each configuration overpressure be established. The generation of these environments was under the direction of Fred Laspesa (Rockwell International); and the determination of resulting loads was under the direction of Ralph Gatto (Rockwell International).

Forcing functions were required in both the pitch plane and yaw plane. In the splitter plate configuration discussed earlier, only pitch plane forcing functions could be obtained. In order to get yaw plane forcing functions, the splitter plate had to be removed above the MLP, necessitating re-establishing an STS-1 baseline, as well as generating the yaw plane environments. The two environments derived in this fashion were then applied to the vehicle simultaneously. Obviously, this is a conservative approach, however, it reduced drastically the complexity of the analysis and the number of load cases required for verification. Looking again at Table 4, tests 19, 20, 27, and 28 were the

pitch plane STS-1 baseline and tests 29 and 30 the yaw plane STS-1 baseline. The STS-2 pitch plane baseline was established by tests 24, 25, and 26, and the yaw plane baseline by tests 31, 32, and 33. Tests (numbers 12, 21, 23, 34, 36, and 38) also helped analysts separate the effects of water injection from the effects of covers used for containment. Of these, test 21 had a different water injection system and was run initially to determine the effect of injecting more water. Where the secondary fix was altered by using soft covers in both the primary and secondary holes, the pitch plane forcing function was re-evaluated for soft covers and found to be very near the environments of the hard covers (tests 36 and 37).

Test 21 was included to see if more water would be effective. This test showed variable results dependent on location of measurement from no basic effect to some increase in overpressure by using more water. Obviously, the water injection system used is not optimum. Test 22 was instituted to recheck the effects of SRM nozzle extension. Again, there was little effect. The mixture between covers only, water only, and water plus covers only (tests 23, 24, 25, 26, 35, 36, 37, and 38) showed that water plus covers was the most effective fix. Covers alone showed between 30 and 50 percent reduction; whereas, water alone reduced levels by 60 percent. The two systems together gave a 67-percent reduction.

The amount of open area in the primary hole is a good indicator of the amount of overpressure suppression; the reduction is proportional to the square root of the area of the opening or the effective diameter of the open area. Figure 33 is a plot of the average overpressure versus percentage of open area.

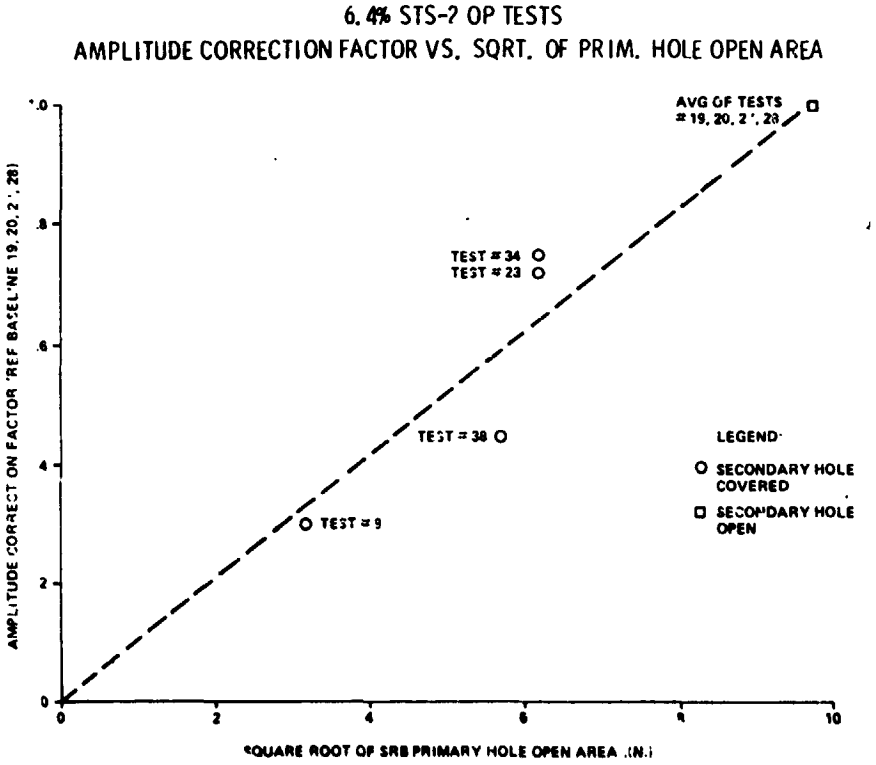

Figure 33. Overpressure reduction versus effective diameter of opening in primary hole.

Comparing the results of Phase I testing versus Phase II testing leads to an interesting observation. The STS-2 fix configuration reduces the overpressure levels below the MLP by 50 percent versus the parametric water system in tests 10 through 18. The levels above the MLP, however, are equal.

At the present time, there is no clear-cut explanation of this difference. Normally, one would expect the values above the MLP to drop by the same ratio as those below. One possible explanation is the change in air volume and the increase in the size of the opening into the SSME hole created when the crest water is lowered after test 18. The logic for the air-volume effect follows from the results when the crest water was turned down (test 15). These results are shown in Figure 34.

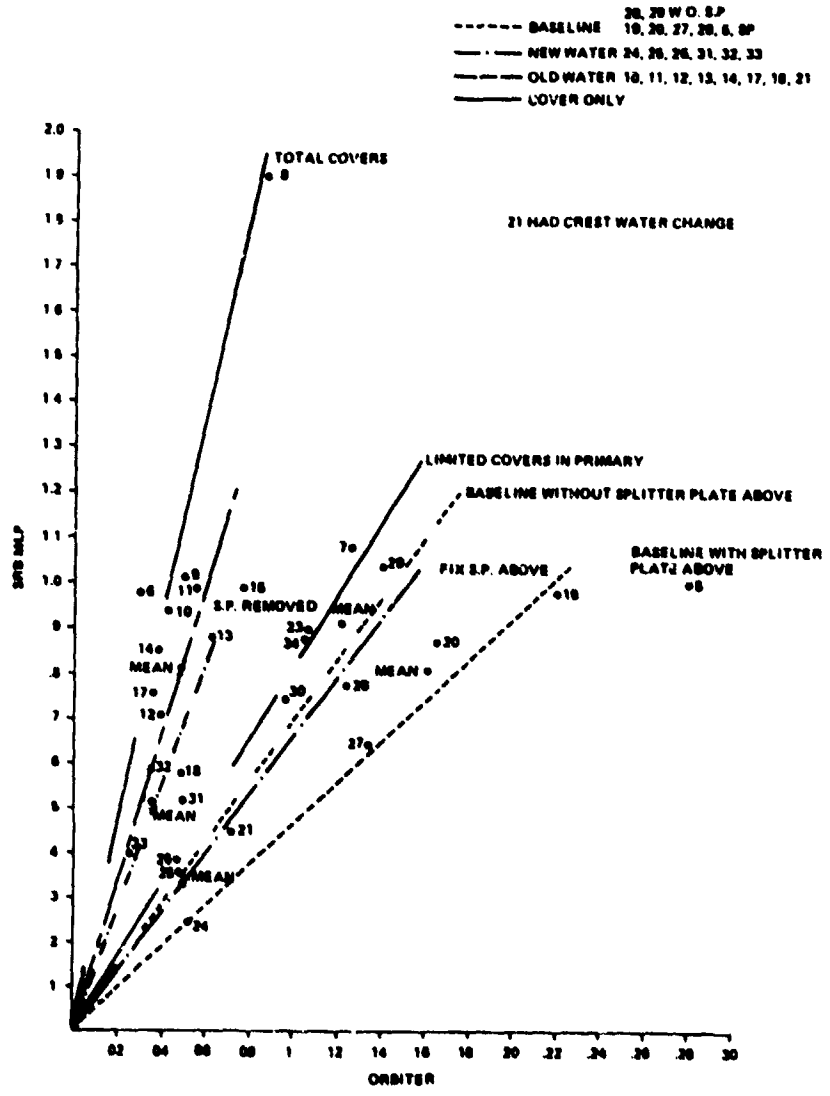

Figure 34. Overpressure above and below MLP.

A summary of the test program and a collection of all the test data are given in References 5 and 6. Anyone desiring a comprehensive set of data should obtain these references.

G. Test Results

The results of the scale model tests can be summarized as follows:

- The primary path of overpressure to the vehicle is through the primary hole.

- Covers over the primary hole increase levels below the MLP and decrease levels above MLP; energy is contained below the MLP.

- Maximum reduction possible with plates (covers) is a factor of four.

- Hard divider between SRB and SSME holes does not affect the Orbiter thermal curtain.

- Louvers in the side deflector cut levels below MLP by a factor of two even if $\dot{P}_c$ is nominal.

- Aiming the crest water down from the horizontal aggravates overpressure.

- Using a splitter plate above the MLP had a negligible effect.

- Consistency of data for each fix is very good. Data have been cross-plotted and analyzed many ways to show this.

- Water injection reduces the source level and thus reduces overpressure levels both below and above the MLP by a factor of three. Water injection has three kinds of effect: blocking the opening, changing the density of the plume, and changing the momentum of the flow.

- Water injection plus covers increases the levels of overpressure below the MLP with some decrease of levels above the MLP relative to water alone.

- Test results indicate more optimum water mixing is possible.

- Water reduces test-to-test data spread.

- Using covers and water is additive for the new configuration. Results of tests 21 and 35 multiplied by results of tests 23 and 34 give results of tests 24, 25, and 26 (i.e., if water alone gives 0.4 X baseline and covers give 0.7 X baseline, then water + covers gives 0.7 X 0.4 = 0.28 X baseline).

- The STS-2 fix gives an overall overpressure reduction of a factor of three.

- The use of covers without water provides only a 55-percent reduction for STS-2.

- Not blocking the north side of the primary hole reduces effectiveness of cover.

- There is good correlation between amplitude and frequency with motor $\dot{P}_c$.

- $\dot{P}_c^2/\overline{P}_c$ scaling predicts STS-1 values higher than mean of $\dot{P}_c$ scaling, but there is less spread in the prediction.

- The modified Broadwell and Tsu model adequately predicts STS-1 overpressure levels using 6.4 percent single motor (with splitter plate) results. Only Orbiter heat shield data do not fit this model.

- Additional options for reducing overpressure environments for subsequent flights are as follows:

- Reducing SRM $\dot{P}_c$ (under study in SRM Project).
- Optimized water injection.
- Slotted side deflector.
- More accurate scaling predictions (reduces tolerances).

One additional factor, how to treat the data scatter, is important to the final loads. Rockwell did a statistical analysis of the Titan data, 6.4 percent scale model data, and SRM hot-firing data. Because of the small sample size, the student T distribution factor was used in handling these data. This is summarized in Table 11 for both a 2σ- and 3σ-level. Using a water scaling uncertainty of 1.25, the final uncertainty factor was obtained for multiplying the nominal value for generating loads. These factors become 2.6 for the 3σ case to be used on heat shields or elements designed by overpressure alone, and 1.8 (2σ) for all elements designed by several liftoff parameters. In this case, a 2σ worst-on-worst parameter spread dynamic analysis is conducted. Mario Rheinfurth (MSFC) has done an extensive statistical analysis of the 6.4 percent model data. His work in this area is outlined in Appendix D.

TABLE 11. COMPARISONS OF SRM IGNITION OVERPRESSURE UNCERTAINTIES

METHOD	$\frac{\text{MEAN} + 2\sigma}{\text{MEAN}}$ (FORCING FUNCTION)	$\frac{\text{MEAN} + 3\sigma}{\text{MEAN}}$ (HEAT SHIELD)	COMMENT
MATH MODEL	1.32	1.40	BASED ON SRM 2σ, 3σ IGNITION TRANSIENT CHAMBER PRESSURE
TITAN III FLIGHT DATA	1.42	2.20	50 Hz LPF OVERPRESSURE DATA MEASURED DURING TITAN III C-25, C-30 & E-05 LAUNCHES
SSLV 6.4% MODEL SINGLE MOTOR TEST DATA	1.50	2.43	BASED ON 6.4% MODEL TESTS CONDUCTED AFTER JULY 1, 1981
RMS OF ALL	1.44 *(1.80)	2.06 *(2.60)	RMS VALUES OF RESULTS FROM MATH MODEL, TITAN III FLIGHT DATA, & SSLV 6.4% MODEL TEST DATA

*WATER SCALING FACTOR WAS ASSUMED TO BE 1.25

SECTION V. FLIGHT RESULTS AND FURTHER CONSIDERATIONS

A. Flight Results

Results from STS-1 flight have been evaluated in detail and generally agreed to by all concerned. Limited STS-2 data were available at the time of publication of this report. The following is a very tentative assessment of the full-scale effects of the suppression system developed using the scale model.

Almost 40 overpressure measurements (Statham gages) were made on the mobile launcher for the first two Shuttle flights. The five measurements indicated in Figure 35 are used in comparing OP data from the baseline and suppressed cases, i.e., STS-1 and STS-2, respectively. Final high-frequency (broadband) STS-2 data are not yet available, which could change these results but not the general trend. Figures 36 through 39 illustrate the effects of the suppression devices on the overpressure produced on the ML. When the overpressure levels are low as for STS-2, they are immersed in the Shuttle Main Engine acoustics and become more difficult to read with great accuracy. Timing events are more difficult to pinpoint; and although the impact on the flight is diminished, they still demand intense academic interest and will be performed at a later date.

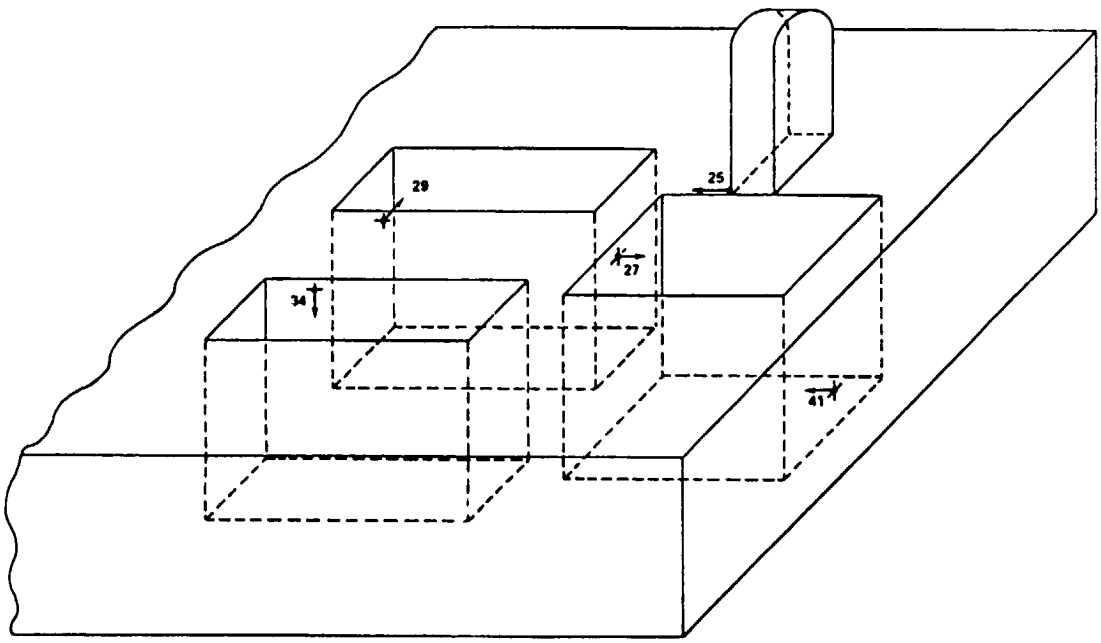

Figure 35. Mobile launcher OP measurements.

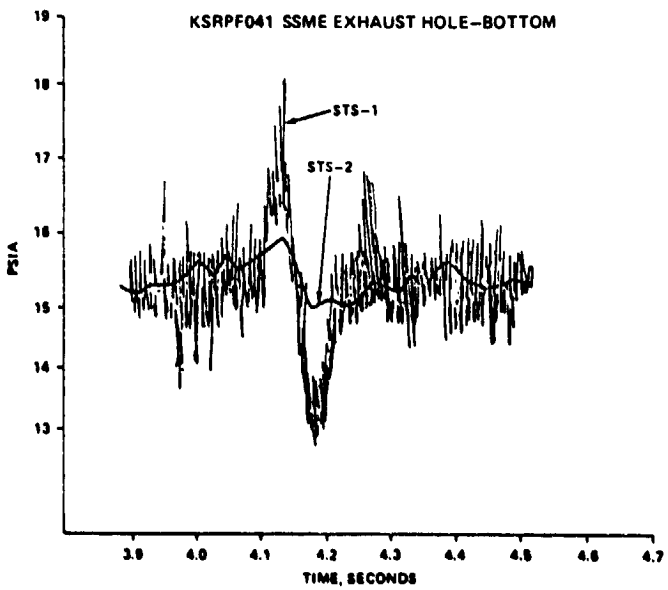

Figure 36. Shuttle overpressure data on LC39 launch facility.

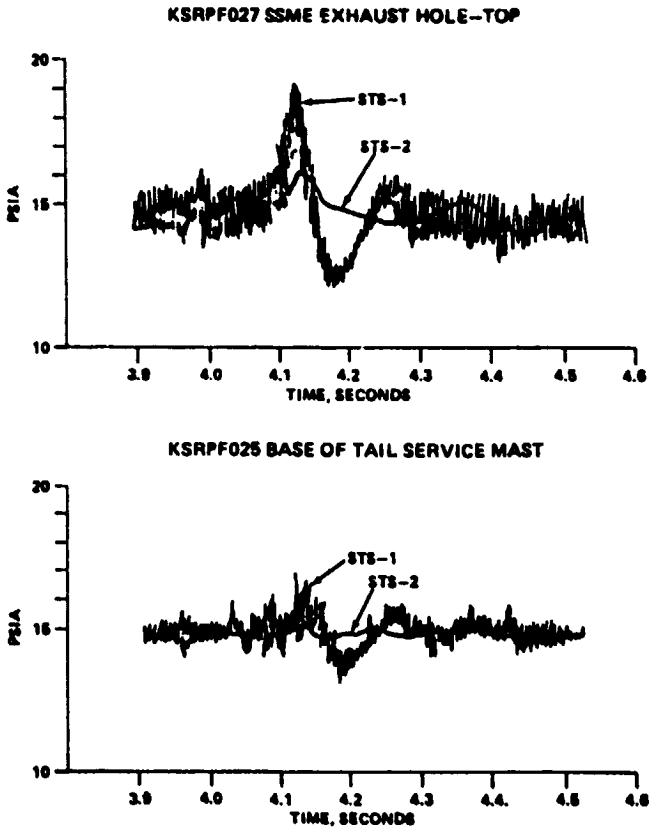

Figure 37. Shuttle overpressure data on LC39 launch facility.

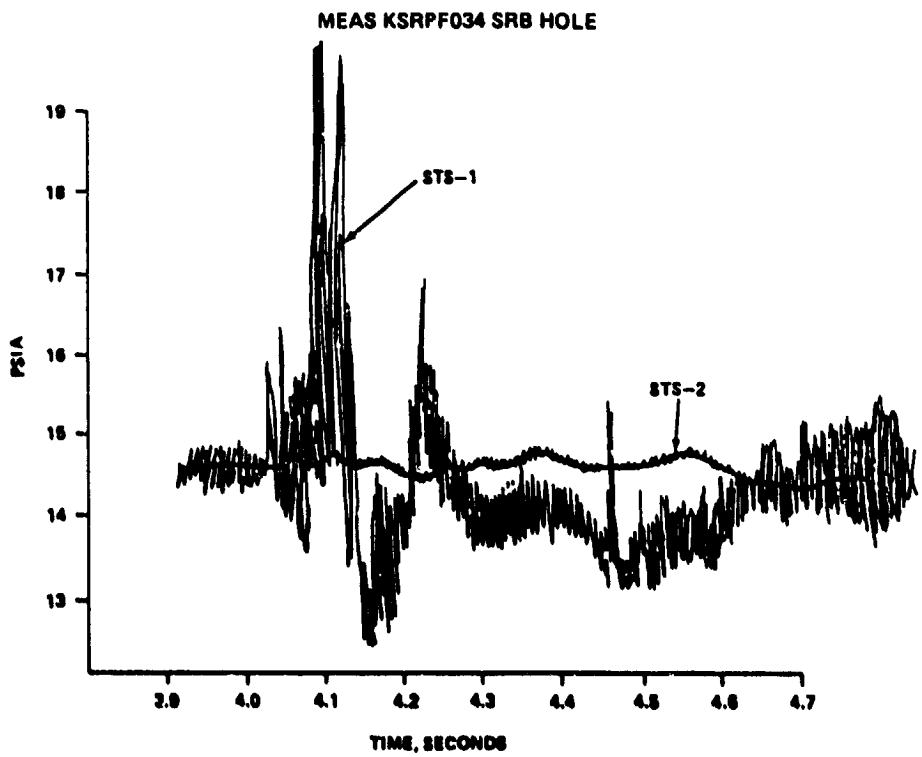

Figure 38. Shuttle overpressure data on LC39 launch facility.

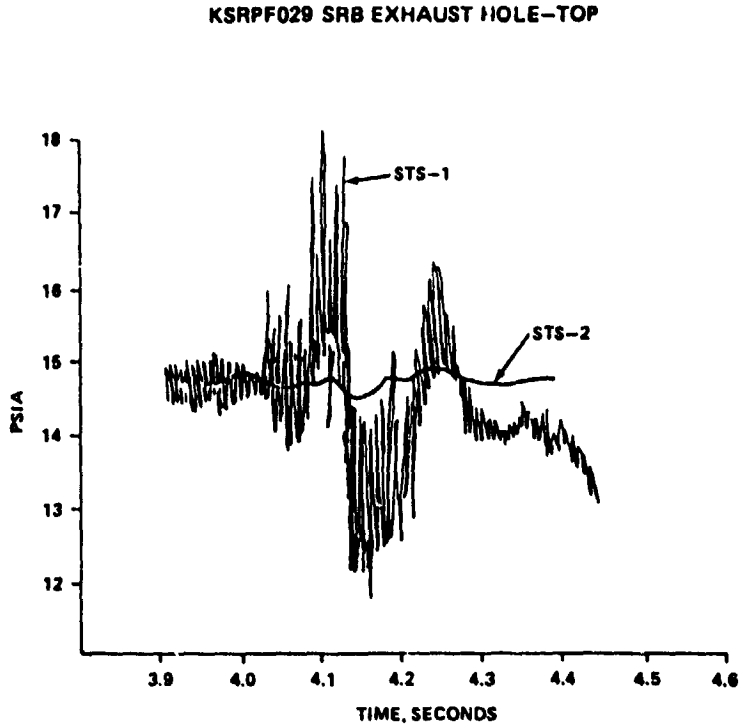

Figure 39. Shuttle overpressure data on LC39 launch facility.

An OP measurement of great interest because of the potential impact on the vehicle is in the center of the Orbiter aft heat shield (between SSME's). On STS-1, the 0 to 400-Hz filtered peak positive overpressure was near 2.5 psi with a rarefactive peak near 2.0 psi, relative to atmospheric pressure. On STS-2 with suppression devices, the level is about 0.25 psi. For vehicle response applications, the OP data are usually filtered 0 to 25 Hz where the STS-1 level was about 1.5 psi versus 0.16 for STS-2, reduced by a factor of nearly ten (Fig. 40).

It should be noted that the data analyses herein are still preliminary for STS-2 data, and will be verified via investigative and rechecking efforts between MSFC, JSC, Rockwell, and KSC instrumentation and data reduction elements.

B. Conclusions

Regarding measured OP data on the launch facility (ML), Figure 41 illustrates both STS-1 measured data, ranging from about 1.3 psi on the tail service mast (highest elevation on ML) to about 4 psi on the bottom of the ML and possibly up to 5 psi. (Data were difficult to validate because of spurious electrical problems and possible transducer responses due to severe thermal inputs.) The data from the same measurements on STS-2 range from about 0.2 psi to about 2 psi on the bottom of the ML, or a reduction of more than two from the baseline configuration and as much as five for some measurements. (Note: STS-2 data are preliminary.)

The overpressure environments for the Orbiter are compared in Figure 42. Results from the 6.4 percent model SSV baseline test compared favorably with STS-1 results. Using the "fixes" on the model STS-2 yielded a factor of three reduction of the overpressure level on the vehicle and is thus

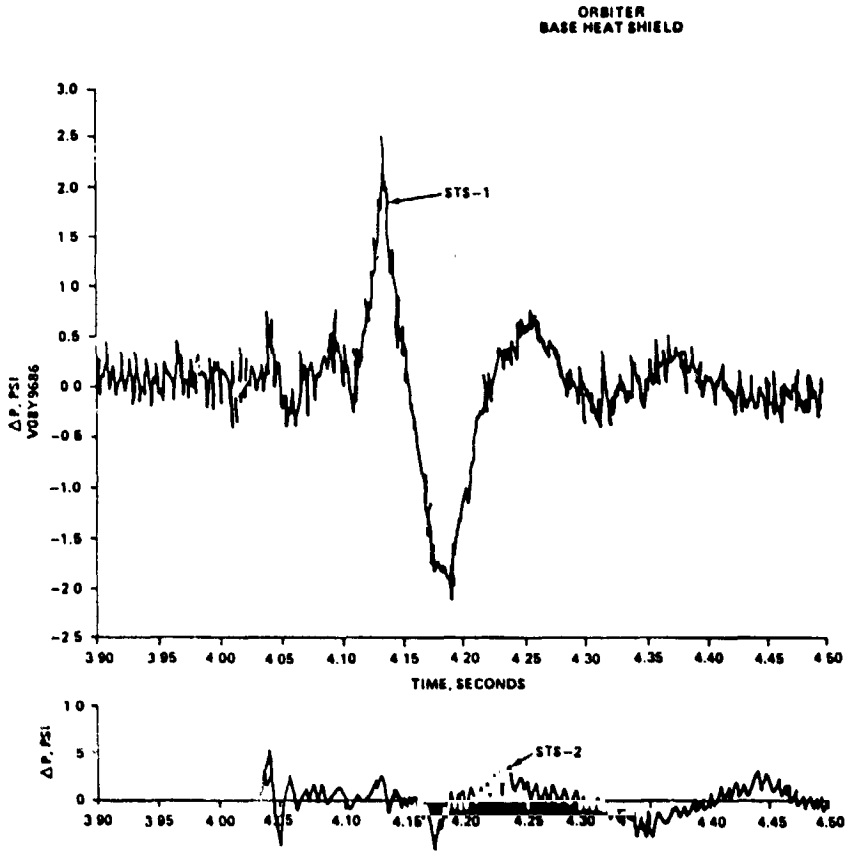

Figure 40. OV102 development flight instrumentation data.

noted in Figure 42. The measured flight overpressures from STS-2 are below the model predictions. This improved suppression on launch may be due to improved water mixing with the exhaust flow. However, it will require some effort to define the exact differences in the model and full-scale data.

It is very important to the Shuttle launch system and future missions that suppression of the overpressure environments was accomplished. The exact description of the phenomenon involved is being addressed, and a more effective suppression without use of covers will probably result for applications to both Eastern Test Range and Western Test Range configurations.

Finally, independent system approaches are very important to achieving good designs. The MSFC independent team activities uncovered several problem areas, any one of which could have led to a mission failure or loss of the vehicle.

C. Future Efforts and Needs

While it is clear from STS-2 that water was able to suppress the ignition overpressure wave, it is not clearly understood by what physical mechanisms the overpressure wave was suppressed. It is likely that the water, through complex transport processes such as momentum, heat, and mass transfer, is able to cool the hot mass of gases from the SRB exhaust which drives the overpressure wave. It is also likely that this wave is further attenuated to some degree as it propagates through the complex mixtures of exhaust gases, steam, and water droplets. If the suppression system for future Shuttle launches is to be optimized, a more basic understanding of the fundamental physical

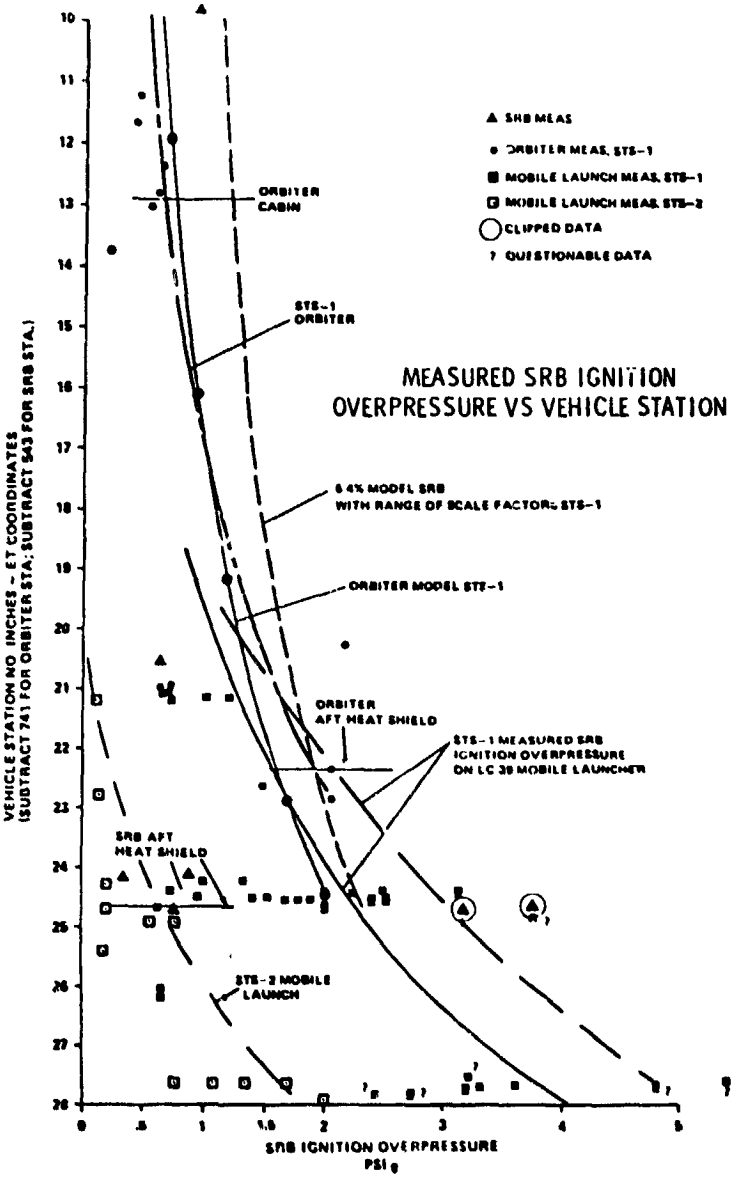

Figure 41. Measured SRB ignition overpressure versus vehicle station.

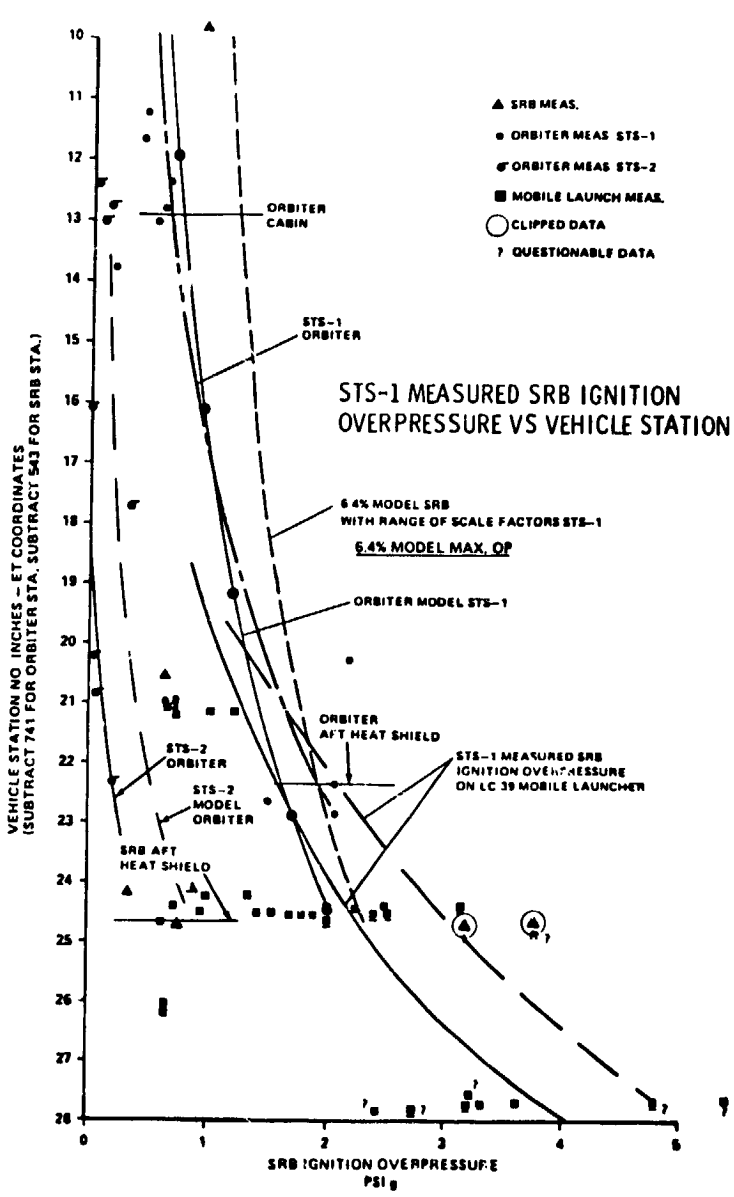

Figure 42. STS-1 measured SRB ignition overpressure versus vehicle station.

processes affecting the generation and propagation of the overpressure wave must be gained. For example, if the size and location of the water droplet cloud in the SRB gas stream are important variables, then it is important to determine an optimum size distribution and to devise a water delivery system which would interact with the SRB gas flow and create this optimum droplet cloud at the right location in the flow. The STS-2 water delivery system was a side injection system in which the water did not have sufficient momentum to penetrate to the supersonic core if the SRB flow had been fully developed. Other means of delivery are being studied, such as high velocity side injection, injection by nozzles placed directly in the flow, etc. Earlier efforts involving water injection into turbines are being investigated for application to rocket overpressure suppression [7,8], and tests will be conducted to verify predictions.

Other more unconventional derivatives of the basic STS-2 water suppression system would involve aqueous foams or carbonated water systems. The aqueous foam can be thought of as a way of preparing the water in a thin-film cellular structure so that microdrops of water are easily formed. It is likely that the interaction of foam with the exhaust stream could produce smaller microdroplets more quickly than by side injection of water alone. Foam has the additional feature that it can be placed in the SRB nozzle or exhaust duct minutes before ignition so that it could fill the nozzle bell and be at rest before the ignition command is given. Of course, it can also be delivered by high pressure hoses into the SRB flow. Various applications of foam have been reported [9-14] with apparent success, and study will continue to address this as a possible fix for Shuttle launch uses.

It may also be possible to pressurize the water delivery system before launch with a gas, such as carbon dioxide (carbonation). Then, as the water system is activated and water flows through the nozzle, it encounters ambient pressure; and the gas comes out of solution, creating bubbles. This water gasification process should also enhance the creation of microdroplets of water, as well as increase attenuation through viscous damping, because the air bubbles and the liquid water possess different internal flow vibration response characteristics when the overpressure wave travels through.

Other means of OP reduction may be through the use of shielding by externally localized coaxial flows used for sound attenuation [15]. Variations of these types of injections, shielding, etc., are also being investigated on a screening level basis with the practical aspects being considered, specifically with regard to launch scale systems [16]. Research and testing will be required to define and understand the phenomenon, and then to optimally apply the results to rocket systems.

APPENDIX A. SIMPLIFIED BROADWELL/TSU MODEL

The Broadwell/Tsu model is based on a semi-empirical theory of the overpressure wave formulated originally to describe the overpressure characteristics for a missile fired in a silo or semi-infinite duct. Observing the MLP and flame trench configuration shown on Figures 5 and 6, one can see the similarity of the configuration to a semi-infinite curving duct. In essence, this theory proposes that the accelerating exhaust particles compress the air contained in the duct, creating shock waves. The shock waves are reinforced by the further acceleration of exhaust gas particles. In addition, it is hypothesized that the overpressure phenomenon is dependent upon thermal effects and afterburning of the fuel-rich propellant gages. These effects are not analytically incorporated, but are rather an empirically determined constant to account for them.

Jess Jones of MSFC applied this basic Broadwell/Tsu approach to the Shuttle configuration with modifications to better explain the Shuttle characteristics and to provide some insight to the basic scaling parameters. His modification accounted for the total Shuttle SRM propulsion characteristics as they related to overpressure. In particular, both an amplitude and a frequency prediction were required, as a function of gas flow Mach number, speed of sound, and action time of mass addition. The following equations describe this modification in terms of scaling parameters as would be applied to the 6.4 percent model data.

A. Amplitude

$$\frac{p^+}{P_o} \sim K_v \frac{\pi}{8} \left[\frac{d}{T_o C_o}\right] M_{o_A} \gamma \quad ,$$

where

d = equivalent diameter of duct

M_{o_A} = Mach number of gas flow into duct

C_o = speed of sound

T_o = mass addition action time = $\overline{P}_c / \dot{P}_c$, where $\overline{P}_c$ is steady-state chamber pressure as a function of time and $\dot{P}_c$ is chamber pressure rise rate

K_v = empirical constant (afterburning, water effects, etc.)

p^+ = positive peak overpressure for entrance to the duct (top of MLP)

P_o = ambient pressure.

B. Frequency

$$f_{FS} = \left[\frac{T_o M}{T_{oFS}}\right] f_M \quad ,$$

where subscript M refers to model and FS to full scale.

The positive peak overpressure at the top of the MLP is a direct linear function of the P_c rise rate. This is inherent in the Broadwell and Tsu model. Consequently, using this modified theory and the Space Shuttle SRM characteristics, the overpressure environment at the top of the SRB opening in the MLP can be predicted. Figure A-1 is a plot of the typical predicted overpressure for the Space Shuttle vehicle. No empirical constant was assumed in this prediction (K_v = 1). This compares quite well with the overpressure wave observed during STS-1 launch.

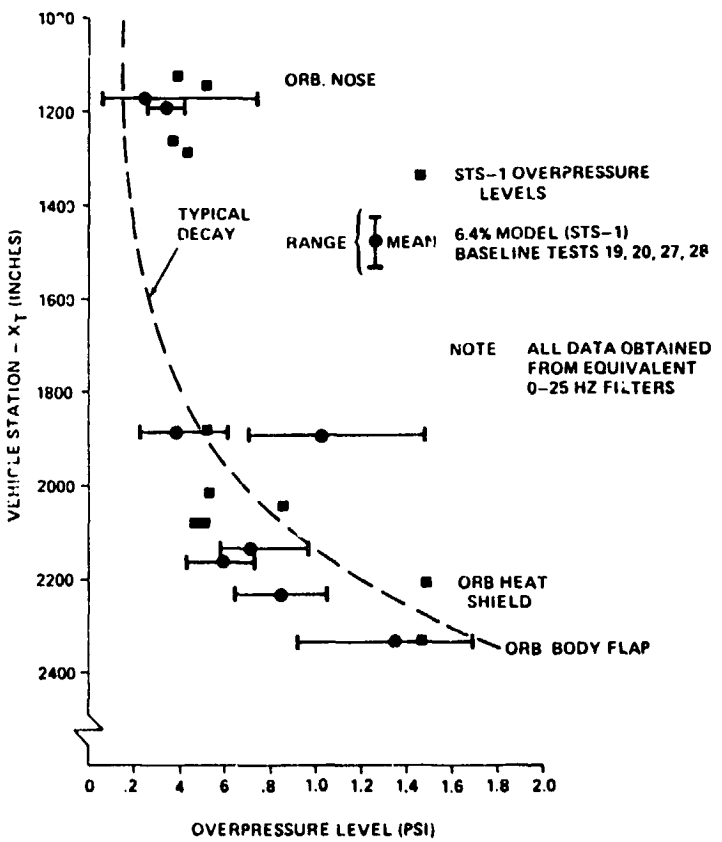

Figure A-1. Comparison of STS-1 overpressure levels with 6.4 percent model equivalent full-scale data.

This theory does not account for the wave decay above the MLP; and, consequently, the model (Broadwell/Tsu) is limited to predictions within the duct. Jones assumes that this decay rate is equivalent to the decay associated with a weak shock wave.

Extending this to scaling up data from the 6.4 percent scale model test is straightforward using the above equations. Figure A-2 shows the scale adjustment factors plotted against chamber pressure

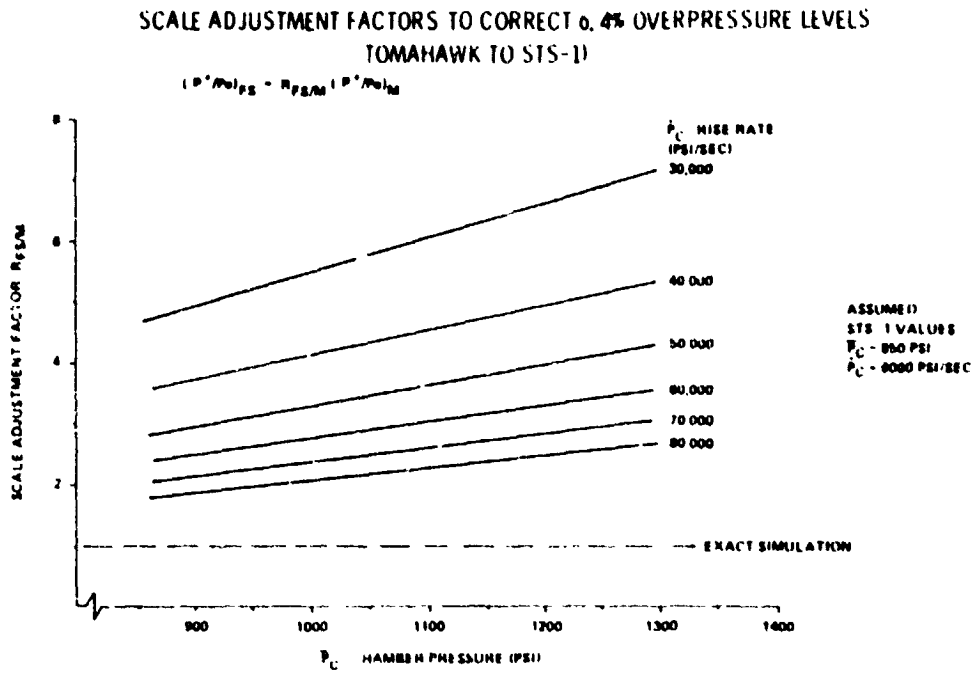

Figure A-2. Scale adjustment factors to correct 0.4 percent overpressure data.

($\bar{P}_c$), with the chamber pressure rise rate ($\dot{P}_c$) as a parameter. The STS-1 values used for this scale factor are shown on the figure: $\bar{P}_c$ = 850 psi, $\dot{P}_c$ = 9,000 psi/sec. This scale adjustment factor accounts for the differences in start up characteristics between the Tomahawk and the Shuttle SRB. This adjustment corrects the 0.4 percent data (at the top of the MLP) to make it equivalent to the STS-1 conditions. It is assumed that the overpressure level experienced by the Shuttle Orbiter, External Tank, and SRB's is a direct linear function of the level emanating from the SRB openings in the top of the MLP. In other words, if the level increased by two at the top of the MLP, then the levels all over the Shuttle also would increase by a factor of two. Within the range of levels obtained from the 0.4 percent tests and those expected from full scale SRB's, this is a reasonable assumption. This then leads to the results shown in Figure A-1. The decay characteristics as shown here are, of course, those determined from the 0.4 percent model data.

This scale factor results, because the 0.4 percent model using the Tomahawk missile does not scale one to one in all key parameters with the Shuttle SRM. This is illustrated in Table A-1, which shows the difference in key parameters. Key differences are in chamber pressure, action time of mass addition, and the thrust rise rate ($\dot{P}_c$). There is a difference in pressure magnitude and waveform, since the second peak of the Tomahawk wave is larger; whereas, the first peak of the Shuttle SRM is much larger than the second.

As mentioned earlier, the $\dot{P}_c$ characteristics determine the fundamental overpressure wave frequency. Figure A-3 is a plot of the frequency adjustment factor versus chamber pressure of the scale model with $\dot{P}_c$ as a parameter.

A comparison of the scale model and STS-1 overpressure, made in the winter of 1979 using the original 0.4 percent scale model data, is shown on Figure 4.

TABLE A-1. TOMAHAWK VERSUS SRM CHARACTERISTICS

	ACTUAL	EQUIVALENT FULL SCALE	SRB
CHAMBER PRESSURE (PSIA)	1200	1200	850
EXIT VELOCITY (FPS)	7500	7500	7627
CHAMBER TEMPERATURE (R^0)	6413	6413	6178
EXIT MACH NUMBER	2.95	2.95	3.00
THRUST	10,600	2,590,000	2,650,000
FLOW RATE (LBS SEC)	43.8	10,694	11,000
SPECIFIC IMPULSE (SEC)	242	242	240.9
EXPANSION RATIO	6.66	6.66	7.16
EXIT AREA DIAMETER (FT^2 FT)	0.396/0.71	96.7/11.1	115.7/12.14
SPECIFIC HEAT RATIO	1.18	1.18	1.18
SPEED OF MASS ADDITION (MACH NUMBER)	2.49	2.49	2.47
ACTION TIME OF MASS ADDITION	0.018	0.29	0.22 (3σ) (PRE DM-1) 0.094 (STS-1)
THRUST RISE RATE ($\dot{P}_C$) (PSIA/SEC)	TWO DISTINCT SLOPES WITH SECOND LARGER		TWO DISTINCT SLOPES WITH FIRST PREDOMINATING

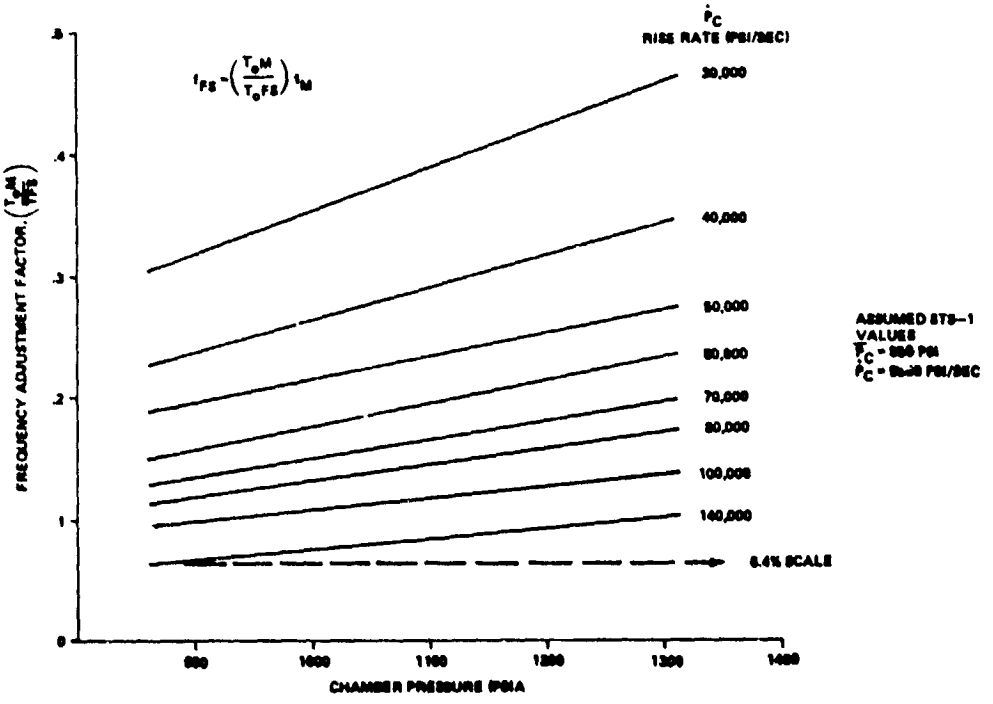

Figure A-3. Frequency adjustment factors to correct 6.4 percent overpressure values (Tomahawk to STS-1).

Jones extended the above analysis to account for the effect of water injection into the SRM plume. This was a simple, one-dimensional approach that considered the mass addition as the only effect present in reducing the overpressure. It is clear that there are other considerations, such as quenching the afterburning, as well as thermal effects, velocity of water injection, and water droplet size. Figure A-4 shows the reduction of over pressure as a function of the mass ratio of injected water to propellant gases. Percent mixing is used as a parameter.

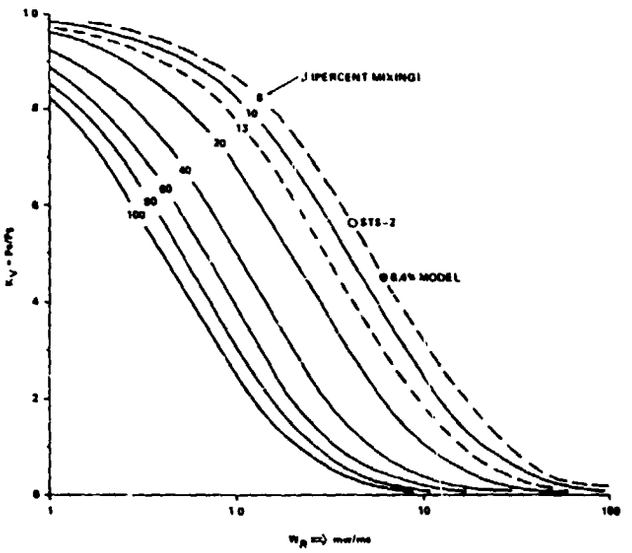

Figure A-4. Equivalent change in density of exhaust flow due to addition of water.

STS-2 and the 6.4 percent ratios are plotted on the curve using the reduction of the scale model as key. This means, obviously, that the water injection approach used is not optimum. Only 8-percent mixing was achieved. Figure A-5 plots the overpressure reduction versus the water mass flow rate divided by propellant flow rate. In this case, mixing is again used as a parameter. Three scale model test results for different water flow rates are plotted using O, Δ, □, and ∇ . A curious thing occurs in that 40,000 gpm of water gives the same result as 70,000 gpm and more reduction than 105,000 gpm of water. Obviously, the total effect of water on overpressure is not completely understood; and other parameters, such as droplet size and stream velocity, must be considered.

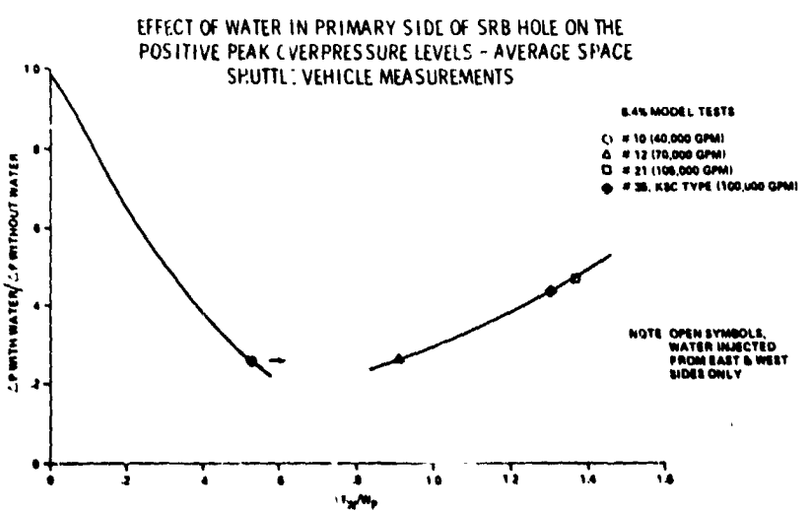

Figure A-5. Effect of water on the positive peak overpressure levels.

APPENDIX B. METHOD OF CHARACTERISTICS

A one-dimensional overpressure model was formulated by H. G. Struck of MSFC. The continuity and momentum equations are solved along certain characteristic lines for which the Riemann variables change in a prescribed manner. The pressure buildup in the rocket case after ignition occurs rather slowly for the first 100 ms. Piston theory rather than combustion theory was used to calculate the trace of the igniter shock wave in the SRM to the throat and nozzle exit. The results were used as initial conditions for the external flow, which is essentially spherical. Figure 40 shows the wave diagram of the external flow and a cross section of the launch facility. The igniter shock leaves the nozzle with a rather small overpressure. At the nozzle exit, it forms a spherical wave which penetrates into the quiescent air with acoustic velocity. The pressure wave arrives at the Orbiter body flap at approximately 120 ms after ignition. Soon after the igniter shock has left the nozzle exit, a strong second shock is formed with the tendency to run upstream. This is the shock which will finally develop into the shock structure of the jet. This shock will not form spherical waves and penetrate into the quiescent air. The initial shock wave produced by the ignition is traveling downstream toward the reflector. It is reinforced by the increasing chamber pressure of the SRM, which reaches the shock front via fast running waves. A reflection pattern is shown in Figure B-1, indicating an arrival of a reflected shock of the body flap approximately 200 to 220 ms after ignition. The reflected shock runs at acoustic velocities or slightly faster, depending on the pressure jump of the shock. The general validity of this model was ascertained by comparing its results with measured pressure responses on the Orbiter wing.

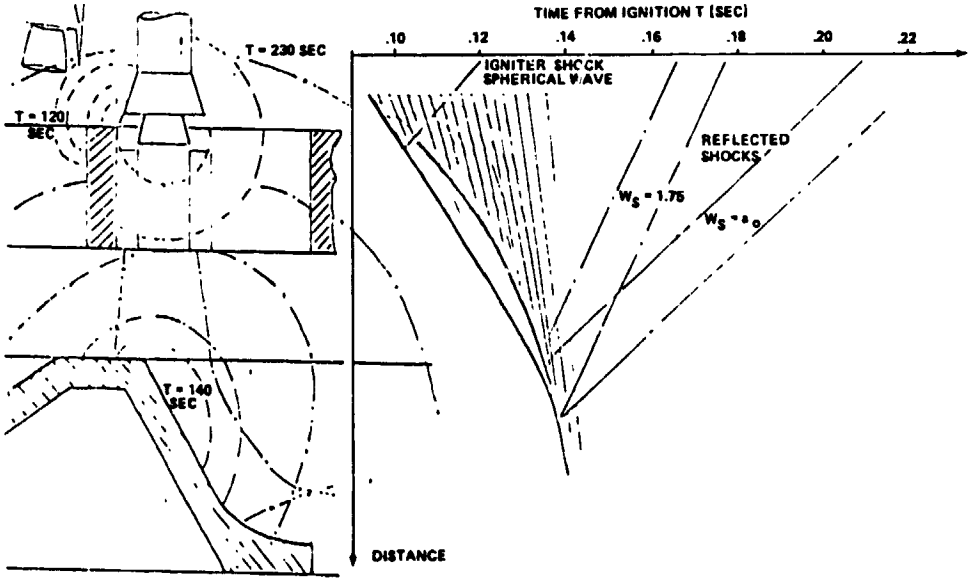

Figure B-1. Wave diagram of the external flow.

The mathematical derivation of similarity laws in closed forms proved to be impossible even with the introduction of drastic simplifications into the basic equations. A numerical approach was, therefore, undertaken to show the dependency of the overpressure on several critical parameters. An excerpt of the result is shown in Figures B-2 through B-4 for a "sawtooth" pressure pulse. The dependence of the overpressure ΔP on the rise rate P_C' for different initial shock pressures P_I at a fixed distance x/x_0 are shown in Figure B-2. The overpressure as a function of P_C' with the distance

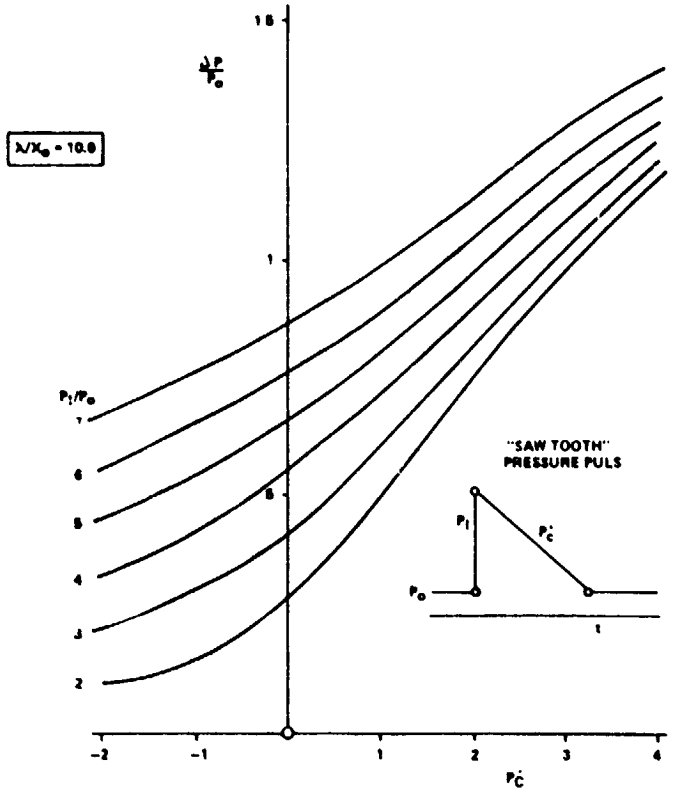

Figure B-2. ΔP dependence on P'_c at x/x_o = 10.0 for different initial pressures P_i.

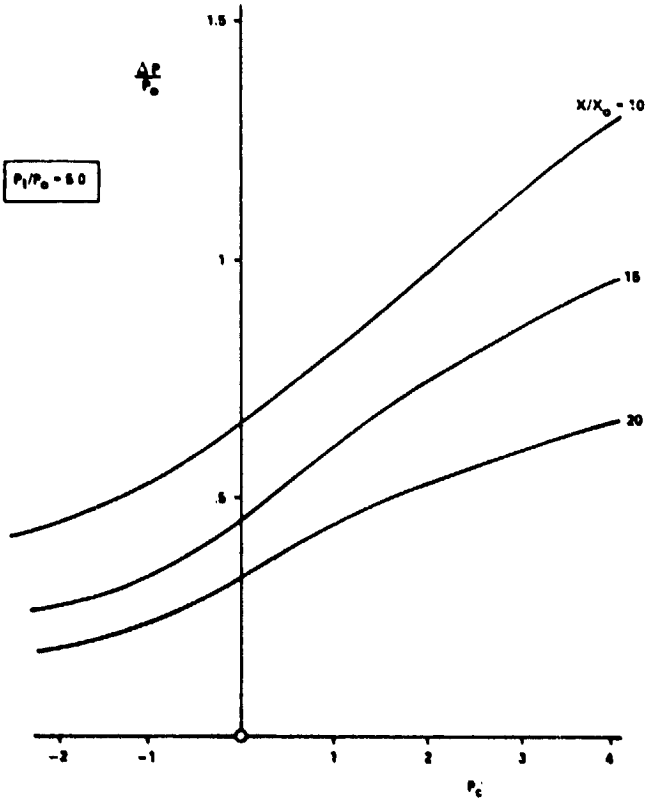

Figure B-3. ΔP dependence on P' for P_1/P_o = 5.0 with distance x/x_o as parameter.

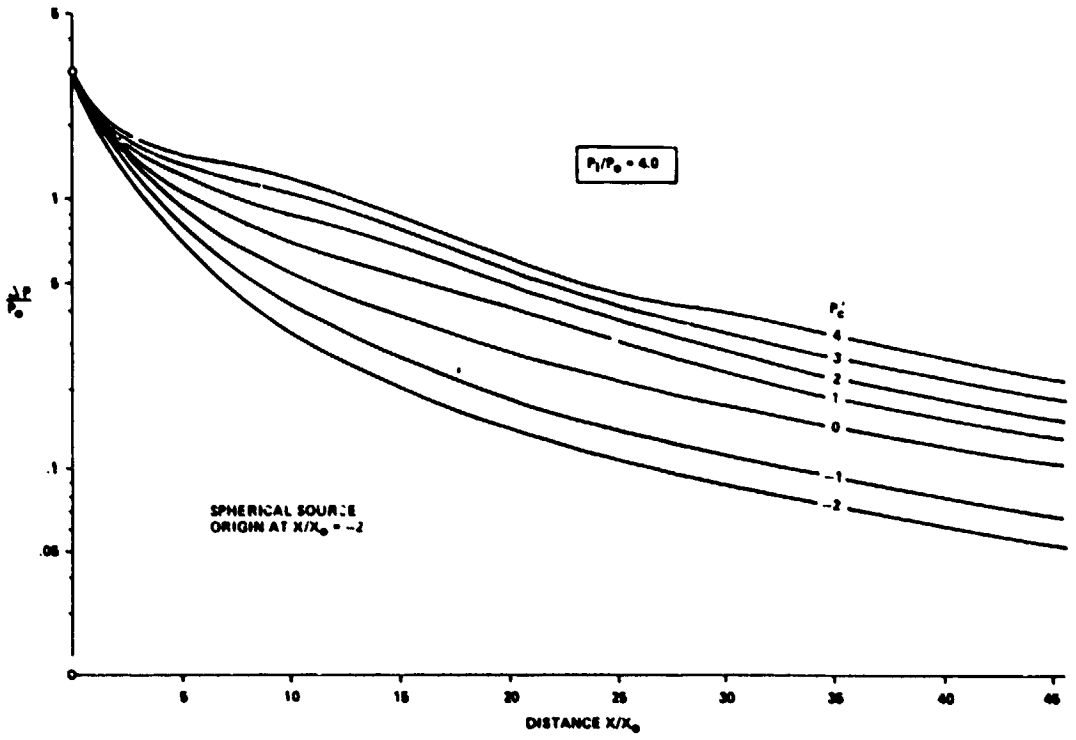

Figure B-4. ΔP decay for P_I/P_O = 4.0 and several P_C'.

x/x_O as a parameter for a fixed initial pressure is depicted in Figure B-3. The overpressure decay for several parameters is shown in Figure B-4. These few examples illustrate the rather complex nature of the overpressure problem.

A simple analysis was conducted to find the effect of adding water to the hot jet. The mixing of two jets with vastly different enthalpies will produce a jet which has lost a certain amount of energy. The resultant apparent chamber pressure is consequently lower and so is the overpressure of the shock wave produced by the apparent chamber pressure. The approximate overpressure reduction as a function of mass ratio and completeness of mixing is shown in Figure B-5, with some test results superimposed. The increase in overpressure for large mass ratios, $\dot{m}_2/\dot{m}_1 > 1.0$, seems reasonable. The mixing becomes largely incomplete, and the gas jet reflects on the water. This effect is not incorporated into the simplified analysis.

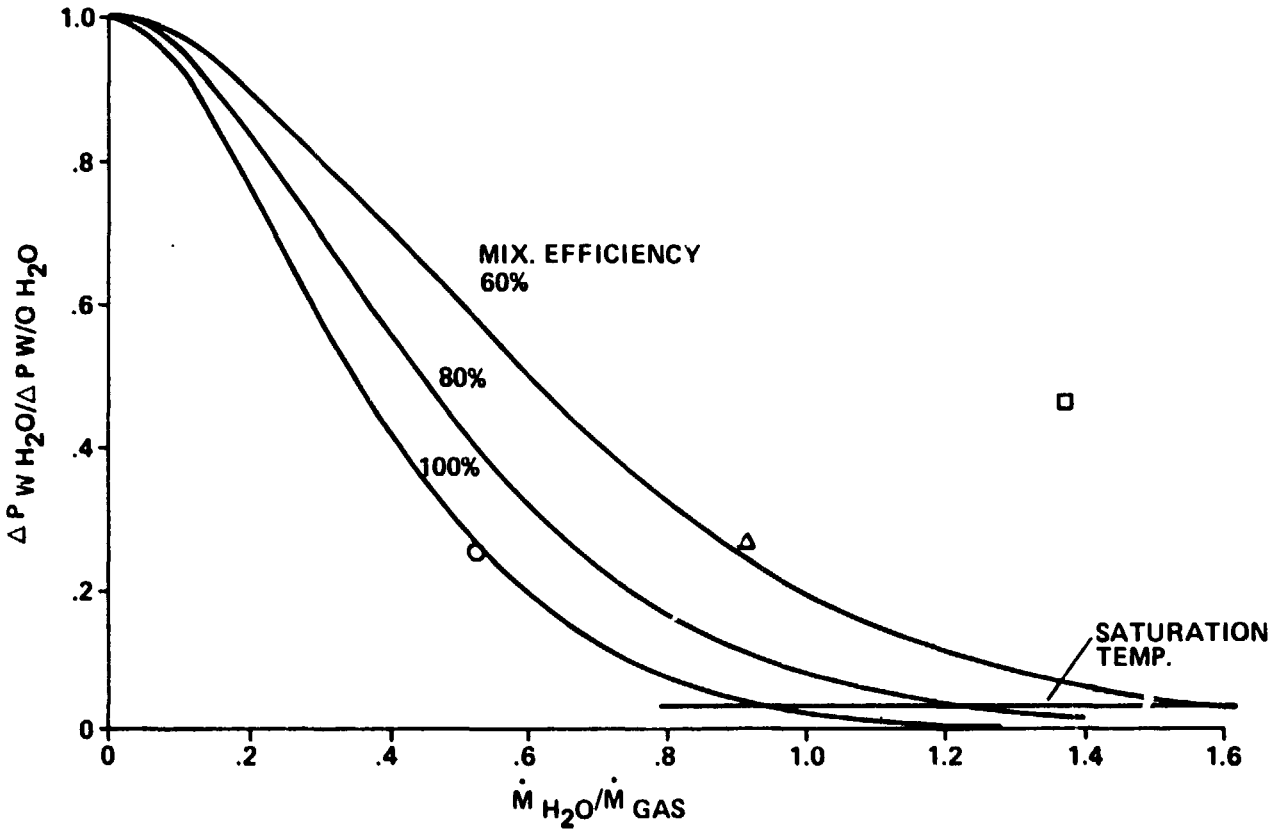

Figure B-5. Overpressure reduction due to water addition.

APPENDIX C. BLAST WAVE THEORY

Dr. Bob Ried has formulated two approaches that have one-, two-, and three-dimensional solutions. One was the blast wave equivalents of the overpressure wave generation by assuming a point of energy source based on the SRM characteristics and an equivalent TNT charge. By plotting the wave propagation within and above the MLP, he attempted to show that the waves above the MLP follow the three-dimensional blast wave theory, depending on distance from the source. This approach did not work. As a result of this work, he reformulated the problem as an iso-intropic gas dynamics problem and fit the data as a function of 1/R, and then non-dimensionalized it in terms of STS-1. This solution provided a good fit to the data. Section IV summarizes the results of Ried's analysis. Key parameters in his analysis are as follows: ΔP, overpressure; P_c, chamber pressure; $\dot{P}_c$, chamber pressure rise rate; A, area; a_{∞}, speed of sound; h_e, enthalpy; and r, distance. Again, this approach shows the same key parameters as the other approaches. The relationships are different and give an improved correlation between the scale model and full scale results for the dry condition over the other approaches. See Section IV for results.

As mentioned previously, in early 1975 at the initiation of the 6.4 percent overpressure program, Scott and Ried developed an analytical model less restrictive than the Broadwell and Tsu approach to describe the ignition overpressure phenomenon. By solving for conditions ahead of and behind the contact surface, the magnitude of the overpressure pulse can be calculated. This model is analogous to the Broadwell and Tsu in that its general characteristics are associated with a piston-type action.

Ried's recent blast wave analysis serves to illustrate the diversity of opinion as to the fundamental nature of complex thermodynamic characteristics associated with the development of the overpressure wave phenomenon and the attempt by the overpressure community to address this complex phenomenon. This blast wave model is under further study by this community.

APPENDIX D. STATISTICAL ANALYSIS OF DATA

The test hypothesis, claiming that a significant reduction of the overpressure can be achieved by these modifications of the launch facilities, was verified via a two-way analysis of variance. The two sources of variability selected for the analysis of variance were the different test configurations and the locations of the pressure transducers. After a preliminary ranking of the different test configurations in terms of overpressure reduction efficacy, the most promising test configurations were singled out for closer inspection. This set of "fix" configurations comprised tests 24, 25, and 26, all of which employ water injection at a rate of 100,000 gal/min. Arranging the mean pressure levels in increasing order of magnitude yields Table D-1.

TABLE D-1. MEAN PRESSURE LEVEL FOR "FIX" TESTS (TESTS 24, 25, AND 26)

Test No.	25	26	24
Mean	0.0584	0.0626	0.0658

Because of the statistical fluctuations of the mean values, any observed difference between two means is only significant if it exceeds $\delta = 0.0169$ for a 95 percent confidence level. Therefore, the difference between the three means is not significant because they all fall below this value. For comparison reasons, a similar ranking was performed for the mean pressure levels of the "baseline" tests 19, 20, 27, and 28 with the following results:

TABLE D-2. MEAN PRESSURE LEVELS FOR "BASELINE" TESTS (TESTS 19, 20, 27, AND 28)

Test No.	28	27	20	19
Mean	0.141	0.151	0.201	0.261

The least significant difference for these means is $\delta = 0.040$ (95 percent confidence interval). This means that only tests 28 and 27 show no significant difference, whereas tests 20 and 19 are significantly different from these and from each other. The cause of this discrepancy between the tests could be some other not yet identified source of variability. Of particular interest would be to reexamine the test data of test 19 which shows the highest significant difference.

The overall overpressure reduction factor can be calculated by dividing the grand mean of the "fix" tests

$$\bar{x}_F = 0.0623$$

by the grand mean of the baseline tests

$$\bar{x}_B = 0.189.$$

The result is:

$$R = \frac{0.0623}{0.189} = 0.33 \quad .$$

Using the experimental errors of both the baseline and the "fix" test configuration, which can be obtained from the corresponding analysis of variance, allows the calculation for an approximate confidence interval for the overall reduction factor. For a 99 percent confidence level, we obtain then

$$0.254 < R < 0.406 \quad .$$

In conclusion, the statistical analysis confirms that, for the 6.4 percent scale model test series, a significant reduction of the overpressure pulse can be achieved by selecting the proper test configuration. The best results were obtained for the test series which employs water injection to the exhaust system.

REFERENCES

1. Atlas E and F Missile Series Launch Environment, Pressure Pulse Analytical Model Studies. General Dynamics/Astronautics, GD/A63-0704, September 1963.

2. Broadwell, J. E. and Tsu, C. N.: An Analysis of Transient Pressures Due to Rocket Starting in Underground Launchers. Space Technology Laboratory-Aerodynamic Department Report No. 51, June 1961.

3. Scott, C. and Ried, R.: Rocket Ignition Overpressures Analysis and Computer Code. Structures and Mechanics Division, Thermal Technology Branch, ES 3-75-2, Johnson Space Center, September 1975.

4. Ryan, R. S.; Bullock, T.; Holland, W. B.; Kross, D. A.; and Kiefling, L. A.: System Analysis Approach to Deriving Design Criteria (Loads) for Space Shuttle and Its Payloads. NASA TP 1949 and 1950, October 1981.

5. Dougherty, N. S. and Mansfield, A. C.: Test Summary Report, 6.4%-Scale SRB Ignition Overpressure Screening of Suppression Concepts Using a Simulated "Popper" Source. Rockwell International Report STS 81-0591, August 1981.

6. Dougherty, N. S.: 6.4 Percent Scale Model SSV Ignition Overpressure Testing for STS-2. Rockwell International Report STS 81-0665, November 1981.

7. Shapiro, A. H. and Hawthorne, W.: The Mechanics and Thermodynamics of Steady One-Dimensional Gas Flow. Journal of Applied Mechanics, Volume 14, pp. A317-A336, December 1947.

8. Shapiro, A. H.; Wadleigh, K. R.; Gavril, B. D.; and Fowle, A. A.: The Aerothermopressor – A Device for Improving the Performance of a Gas-Turbine Power Plant. Transactions of the ASME, Volume 78, pp. 617-653, April 1956.

9. de Krasinski, J. S. and Khosla, A.: Shock Wave Provocation and Attenuation in Foams. Presented at 5th Australasian Conference on Hydraulics and Fluid Mechanics, University of Cantibery, Christchurch, New Zealand, December 9-13, 1974.

10. Dadley, D. A.; Robinson, E. A.; and Pickett, V. C.: Use of Foam to Muffle Blast from Explosions. Presented at IEP-ABCA-5 Meeting, NAVEODFAC, Indian Head, USA, June 23-30, 1976.

11. Winfield, F. H. and Hill, D. A.: Preliminary Results on the Physical Properties of Aqueous Foams and Their Blast Attenuating Characteristics. Suffield Technical Note Number 389, Defence Research Establishment Suffield, Ralston, Alberta, August 1977.

12. Clark, A. K.; Hubbard, P. J.; Lee, P. R.; and Woodman, H. C.: The Reduction of Noise Levels from Explosive Test Facilities Using Aqueous Foams. Royal Armament Research and Development Establishment, Fort Halstead Sevenoaks, Kent, U. K.

13. Anson, W. and de Krasinski, J. S.: Field Experiments in the C.I.L. Facilities of the University of Calgary. Mechanical Engineering Department Report Number 76, March 1976.

14. Pater, L. L. and Shea, J. W.: Use of Foam to Reduce Gun Blast Noise Levels. Naval Surface Weapons Center Report Number NSWC TR 81-94, Dahlgren, Virginia, March 1981.

15. Cowan, S. J. and Crouch, R. W.: Transmission of Sound Through a Two-Dimensional Shielding Jet. Presented as Paper 73-1002 at AIAA Aero-Acoustics Conference, Seattle, Wash., October 15-17, 1973.

16. Woo, J., Jr.: Studies Related to 6.4% Model Overpressure Assessment. Gamma Research, Inc., Report GRI-TP-81-10, Contract NAS8-34567, December 2, 1981.

17. Struck, H. G.: A One-Dimensional Approximation to the SRB Jet Exhaust Overpressure Wave. MSFC Memorandum ED31-81-17, July 17, 1981.

18. Salita, M.: Description of the Shock Waves Generated During the Initial Ignition Transient of the Space Shuttle Rocket Boosters. Thiokol Report TWR-13092, July 1981.

19. Jones, J.: Scaling Considerations of the 6.4% Model Overpressure Data. MSFC Memorandum ED24-81-47, August 25, 1981.

APPROVAL

PROPULSION SYSTEM IGNITION OVERPRESSURE FOR THE SPACE SHUTTLE

By R. S. Ryan, J. H. Jones, S. H. Guest, H. G. Struck, M. H. Rheinfurth, and V. S. Vaidyaraime

The information in this report has been reviewed for technical content. Review of any information concerning Department of Defense or nuclear energy activities or programs has been made by the MSFC Security Classification Officer. This report, in its entirety, has been determined to be unclassified.

George F. McDonough
Director, Systems
Dynamics Laboratory